DNA binding and unwinding by Hel308 helicase requires dual functions of a winged helix domain.

Sarah J Northall[1,2], Ryan Buckley[1] Nathan Jones[1], J Carlos Penedo[3,4], Panos Soultanas[2] and Edward L Bolt[1*]

The University of Nottingham, U.K, [1]School of Life Sciences, [2]School of Chemistry.
[3] SUPA School of Physics and Astronomy, North Haugh, University of St Andrews, KY16 9SS, [4] Biomedical Science Research Complex (BSRC), School of Biology, University of St Andrews, KY16 9ST, UK

Correspondence to ed.bolt@nottingham.ac.uk, +44 115 8230194.

Abstract

Hel308 helicases promote genome stability linked to DNA replication in archaea, and have homologues in metazoans. In the crystal structure of archaeal Hel308 bound to a tailed DNA duplex, core helicase domains encircle single-stranded DNA (ssDNA) in a "ratchet" for directional translocation. A winged helix domain (WHD) is also present, but its function is mysterious. We investigated the WHD in full-length Hel308, identifying that mutations in a solvent exposed α-helix resulted in reduced DNA binding and unwinding activities. When isolated from the rest of Hel308, the WHD protein alone bound to duplex DNA but not ssDNA, and DNA binding by WHD protein was abolished by the same mutations as were analyzed in full-length Hel308. Isolated WHD from a human Hel308 homologue (HelQ) also bound to duplex DNA. By disrupting the interface between the Hel308 WHD and a RecA-like domain, a topology typical of Ski2 helicases, we show that this is crucial for ATPase and helicase activities. The data suggest a model in which the WHD promotes activity of Hel308 directly, through binding to duplex DNA that is distinct from ssDNA binding by core helicase, and indirectly through interaction with the RecA-like domain. We propose how the WHD may contribute to ssDNA translocation, resulting in DNA helicase activity or in removal of other DNA bound proteins by "reeling" ssDNA.

Introduction

Hel308 and HelQ are homologous helicases from the Ski2-family that promote genome stability linked to DNA replication in archaea and metazoans respectively. They participate in DNA repair at replication forks (1-9), and interact with RPA and homologous recombination proteins (3,10-13). Hel308 and HelQ are single-stranded DNA (ssDNA) stimulated ATPases that unwind a variety of DNA structures by translocation along ssDNA (1,5,14) and can displace DNA-bound proteins (15). Crystal structures of archaeal Hel308 proteins (15-17) show five-domains, including a three-domain core ATPase-helicase that powers directional (3' to 5') ssDNA translocation, in common with other superfamily 2 helicases (16,18). Hel308 is proposed to "ratchet" along ssDNA by movements of RecA-like domains 1 and 2 relative to ssDNA (16,19). The structure of Hel308 from *Archaeoglobus fulgidus* (16) (and see Figure 1A) is in complex with a 3' single-strand tailed partial duplex DNA, the minimal substrate unwound by Hel308 helicases. There are extensive DNA-Hel308 contacts that encircle ssDNA, positioning it optimally for translocation mediated by a prominent α-helical "ratchet" in domain 4. DNA strand separation is achieved at a β-hairpin located in domain 2. Additional domains 3 and 5 adorn the structural periphery of Hel308; domain 5 makes multiple contacts with ssDNA to modulate ATPase and helicase activities (15,20), and domain 3 is a winged helix fold. This winged helix domain (WHD) has a solvent exposed putative 'recognition' α-helix similar to DNA or protein binding modules in other proteins (21). In the Hel308 structure bound to a 3'-tailed duplex, the WHD makes no contact with DNA, possibly because the substrate used did not extend far enough for binding to be observable. Hel308 helicase shows preference for unwinding forks or D-loops (5,8,22) over partial duplexes, and one possibility was that binding of Hel308 to forks might orientate the WHD close to duplex DNA arms of these or similar substrates. The winged helix domain (WHD) also packs tightly against RecA-like ATPase domain 1, a characteristic of Ski2 helicases generally (18,23). We analyzed the WHD of archaeal Hel308 and observed that it contributes to DNA binding and unwinding activities through residues on a solvent exposed α-helix, and by its packing against RecA-like domain 1. Purified isolated WHD domains from archaeal and human Hel308 and HelQ enzymes bound to duplex DNA, but not to ssDNA. We propose that duplex DNA binding by the Hel308 WHD can promote ssDNA translocation by core Hel308 domains that can be utilized for both DNA unwinding or reeling of ssDNA to remove bound proteins.

Results

Mutation of the Winged Helix domain in Hel308 cause reduced enzyme function

In the structure of *Archaeoglobus fulgidus* Hel308 bound to tailed duplex DNA [AfuHel308, PDB 2P6R (16)] single-stranded DNA threads through core helicase domains 1, 2 and 4 and an accessory domain 5 (Figure 1). A winged helix domain (WHD) does not form significant contacts with this DNA molecule, possibly because the DNA is too short or is unbranched. We investigated if the Hel308 WHD binds DNA, using protein from the archaeal species *Methanothermobacter thermautotrophicus* [(MthHel308)(5)], which has 34% overall identity (3e-93) in amino acid sequence with AfuHel308; Figures S1 and S2 provide sequence alignments and structural comparisons of full length archaeal Hel308 proteins, including from *Sulfolobus solfataricus* (Sso) and *Pyrococcus furiosus* (Pfu), which have been structurally determined without bound DNA (15, 17). Figure 1 highlights part of the Hel308 WHD that we used to investigate protein function; (a) a solvent exposed α–helix, herein called α–20, that contains a conserved tyrosine (Y460), and (b) well conserved phenylalanines (F434 and F439) on the WHD "inward face" that pack against RecA-like helicase domain 1. We reasoned that Hel308 α–20 could be a "recognition" helix for DNA binding in branched substrates, typical of canonical WHDs in many proteins. We first focus on this in Hel308, returning to the phenylalanines later.

The MthHel308 WHD was mutagenized and a genetic assay was used to assess the effect on Hel308 helicase function (Figure 2, and Supplementary results). The assay used *E. coli* strain *dnaE486* Δ*recQ* (24,25) to determine if Hel308 mutants are active (5,24). Briefly, in this strain mutation in DNA polymerase III (encoded by *dnaE*) destabilizes replication forks at 37^{o}C causing poor cell viability, but this is alleviated by deletion of the gene encoding *E. coli* helicase RecQ (Δ*recQ*) (24,25). Re-introducing RecQ from a plasmid restores the poor growth phenotype, an effect reproduced by MthHel308 (5), summarized in Figures 2 and S3. Expression of Hel308 or RecQ (pHel308 or pRecQ) in *dnaE486* Δ*recQ* caused >1000 - fold reduced viability at 37^{o}C compared to a control plasmid (pEmpty). Inactivation of Hel308 ATPase and helicase activity by mutation of Walker A lysine residue (pHel308^{K51L}) restored cells to normal growth alike to pEmpty (Figure 2). We mutated Y460 in MthHel308 WHD α–20, to alanine (pHel308^{Y460A}), because this tyrosine is conserved and has properties that are potentially important for any DNA binding by this part of the WHD. Hel308^{Y460A} gave an intermediate phenotype that was 100 – fold more viable than wild type Hel308, but 100 – fold less viable than K51L, or empty plasmid (Figure 2). The same effect was observed when mutation of Y460 was combined with further mutations by additionally changing Q459 and N464 to glycine, creating pHel308^{QYN}, thus removing each of three most likely DNA binding residues from α–20. Expression levels of each Hel308 protein observed by western blotting

were similar during the assay, summarized in Figure 2, and in the full gel shown in Figure S4, confirming a functional effect of the Hel308 WHD mutations, rather than an effect caused by absent protein expression. The phenotypes of these Hel308 WHD mutant proteins indicated that they were worthy of further analysis.

Hel308 Winged Helix domain mutations reduce DNA binding and unwinding but binding to single stranded DNA is unaffected

Hel308 is a single strand DNA (ssDNA) stimulated ATPase that is most effective at unwinding forked DNA containing ssDNA gaps (5,22). Hel308^{Y460A} and Hel308^{QYN} proteins were purified (Figure S5) and assayed for unwinding forked DNA (fork-2) containing a 25 base-pair duplex and 25 nucleotide ssDNA "flaps" (Figure 3A). Unwinding of fork-2 was reduced by 2 - 4 fold compared to wild type Hel308, measuring helicase activity of Hel308^{Y460A} and Hel308^{QYN} as a function of time (100 nM Hel308; 10 nM DNA). Hel308^{Y460A} and Hel308^{QYN} unwinding of a 3' tailed duplex, the minimal helicase substrate for Hel308, was also reduced by a similar margin as for fork-2 although overall this substrate is unwound less well than fork-2.

Binding by the wild – type and mutant versions of the Hel308 was assessed by fluorescence anisotropy using a FAM-labeled fork-2 substrate. Equilibrium dissociation constants were determined by plotting the change in fluorescence anisotropy in response to increasing concentration of Hel308 (Figure 3B) and fitting it to a quadratic function assuming a 1:1 binding model (details in methods section). Fluorescence anisotropy measurements for wild type Hel308 binding to fork-2 gave a dissociation constant (K_d) of 1.6 nM, which increased to 35 nM and 160 nM for Hel308^{Y460A} and Hel308^{QYN} respectively. It is important to note that the dissociation constant obtained for the Hel308^{QYN} mutant is in excellent agreement with the value reported for wild-type Hel308 binding to a 15-mer single-stranded DNA using an identical anisotropy-based method (~ 140 nM) (15). In the context of the fork-2 substrate, the strong binding preference observed for wild-type Hel308 compared to Hel308^{Y460A} (30-fold) and Hel308^{QYN} (~100-fold) is consistent with a role for the WHD in fork-2 DNA binding, with reduced binding of mutant proteins contributing to reduced helicase activities (Figure 3B).

Two different stable protein-DNA complexes can be observed in EMSAs of wild-type Hel308 binding to fork 2, and the same complexes were observed for Hel308^{Y460A} (5) and Figure S6A. This indicates that although the WHD mutations reduce DNA binding, they do not affect the general topology of fork-2 bound complexes. We also observed no reduction in ssDNA stimulated ATPase activity of either mutant protein, compared to wild type Hel308 (Figure S6B). In summary, genetic analysis and DNA binding and unwinding data for Hel308^{QYN} suggested that the Hel308 WHD is functionally important.

Fork-2 DNA has ssDNA and duplex DNA regions of the same length. In the crystal structure of Hel308 bound to a similar structure, a DNA partial duplex, the core helicase domains 1, 2, 4 and 5 encircle ssDNA *via* many contacts, and additional contacts are made to duplex DNA from domains 2 and 4. However, the partial duplex in this structure does not extend as far as the WHD (domain 3). To further analyze DNA binding defects associated with Hel308 WHD mutations we isolated WHD proteins to assess their binding to ssDNA and duplex DNA in the absence of any DNA binding by domains 1, 2, 4 and 5.

Isolated winged helix domain proteins from Hel308 and HelQ bind to duplex DNA, but not single stranded DNA, and binding is abolished by mutations

The isolated WHD (WHD^{WT}) from MthHel308 was cloned, over-expressed and purified based on amino acid alignment shown in Figure 1B, and on the structure of *Archaeoglobus* Hel308 (Figure 1A, and Figure S7). Purified 11-kDa WHD protein eluted as a peak corresponding to a single folded species within the range of expected size (Figure S8). We then assessed binding of WHD^{WT} to duplex DNA and ssDNA in turn. Titration of WHD^{WT} (0 - 250 nM) into buffer containing 70 base-pair duplex DNA (10 nM) showed a single protein-DNA complex (Figure 4A, lanes 1-5). DNA binding by WHD^{WT} was not sequence specific, being observed on 33bp and 50bp DNA duplexes of different nucleotide sequence (Figure S9). Significantly, introduction into WHD^{WT} of the same amino acid substitutions as in $Hel308^{QYN}$ gave a mutant protein (WHD^{QYN}) that did not form a binding complex with duplex DNA (Figure 4A, lanes 6-9), but the gel filtration elution profile of WHD^{QYN} was the same as WHD^{WT} (Figure S8). Interestingly, WHD^{WT} did not bind to the 70 - nucleotide ssDNA (Figure 4A, lanes 10-13), a substrate that is bound avidly by full length Hel308 (lanes 14 and 15). This difference in binding to ssDNA and duplex DNA is discussed later, in a model for core helicase binding to ssDNA, aided by weaker interaction of the WHD with duplex DNA.

Human HelQ helicase has 25% overall sequence identity to MthHel308 (5)(Supplementary Table 3) but there is no crystal structure available. Sequence alignment with archaeal Hel308 enzymes (Figure S1), and a Phyre2 (26) structural model of human HelQ (Table S3) included a predicted WHD that was used to guide cloning, expression and purification of isolated HelQ WHD protein (Q-WHD^{WT}, Figure S7) for biochemical comparison with Hel308 WHD. Q-WHD^{WT} bound to duplex DNA in EMSAs as a single complex when titrated from 0 to 20 nM of protein (Figure 4B lanes 1-4). Mutations were made within the WHD of HelQ, targeting a tyrosine residue Y818 and a lysine, K819, which were altered to Serine and Aspartate respectively (Q-WHD^{YK}). The mutant protein was unable to bind duplex DNA, even at up to 100 nM of protein (Figure 4B lanes 5-10). We conclude that WHDs from Hel308 and HelQ both bind to duplex DNA.

Interaction of the Hel308 WHD with a RecA-like domain is required for ATPase and helicase activity

The Hel308 WHD is packed tightly against RecA-like ATPase domain 1, a feature common to other Ski2 helicases (18). The interface includes two phenylalanine residues (Figure 1, F434 and F439, using MthHel308 numbering) that are highly conserved in Hel308 and HelQ sequences (Figure 1B and S1). Each was individually changed to alanine or valine in full-length Hel308 proteins to assay for effects on Hel308 function. In the genetic assay, described for Hel308 WHD mutants in Figure 2, F439A Hel308 gave the same phenotype as an ATPase defective Walker A motif mutant of Hel308, K51L, and F434V was intermediate between F434V/K51L and wild type (Figure 5A and S10). Purified F439A Hel308 showed 10 - 50 fold reduced ATPase activity (Figure 5B) and barely detectable helicase activity (Figure 5C), consistent with its phenotype in the genetic test. Activities of F434V Hel308 were reduced relative to wild type protein, but less dramatically than F439A protein (Figure 5C). Despite severely reduced ATPase and helicase activities of F439A, binding of this protein to fork-2 DNA in EMSAs was reduced by about two-fold (Figure S11). The data on the conserved phenylalanines located at the interface of WHD-RecA domain interface suggest important functional cross talk between the WHD and the core helicase motor domains.

Discussion

Hel308 is typical of superfamily 2 helicases in utilizing core ATPase (RecA-like) and ratchet domains for translocating ssDNA (15,16). A β-hairpin in a RecA-like domain separates DNA strands during Hel308 helicase activity and Hel308 is also effective at removing other DNA bound proteins (5,15,16,22), contributing to recovery of compromised replication forks (9). The crystal structure of archaeal Hel308 bound to a partial duplex DNA (16) includes a winged helix domain (WHD) whose function is unknown. Analysis of the WHD here showed that; (a) it binds directly to duplex DNA, but not to ssDNA, requiring residues (e.g. Y460) on a solvent facing alpha helix, (b) it is required indirectly for ATPase and helicase activity, through interaction with a RecA-like domain *via* phenylalanine residues (F434 and F439). Genetic phenotypes consistent with reduced Hel308 function were observed for both sets of mutations. A single mutation in the proposed WHD DNA binding alpha helix (Y460A) resulted in a 35 - fold increase in the K_d for Hel308 binding to a DNA fork, and additional mutation of amino acids in the same helix, creating Hel308^{QYN}, weakened fork DNA binding further still. Reduced unwinding of the same fork substrate by WHD mutants was consistent with reduced DNA binding. These data indicate that the Hel308 WHD contributes to helicase activity by direct interaction with DNA.

The isolated 11.8 kDa Hel308 WHD protein bound to duplex DNA, but not to ssDNA. Binding to duplex DNA by the WHD protein was abolished by mutations that much reduced fork DNA binding in full length Hel308, in which other domains, mainly domains 2, 4 and 5, contribute to ssDNA and duplex binding. Second, Hel308^{Y460A} and Hel308^{QYN} mutations reduced helicase activity at least as much on a minimal substrate, a 3'-tailed duplex, as on a preferred forked substrate. This indicates that the WHD promotes Hel308 helicase unwinding but is not providing specificity for preferred DNA structures. More likely it engages with duplex DNA proximal to ssDNA, which is required for triggering ATPase activity of Hel308 translocation/helicase. Hel308 would therefore have two modes of DNA binding: core helicase binding to ssDNA, and functionally important binding of the WHD to DNA duplex (Figure 6). This is consistent with previous data that Hel308 binds weakly to duplex DNA (5), also observed from the isolated WHD protein in this work. Binding of Hel308 WHD to duplex DNA is compatible with unwinding a 3' tailed duplex DNA, by core helicase domains translocating 3' to 5' and driving DNA strand separation at the β-hairpin of domain 2 (Figure 6A). However, Hel308 may also function by a "DNA reeling" mechanism to translocate ssDNA with a 5' end, the WHD interacting with double-stranded DNA at a duplex – ssDNA junction (Figure 6B). In this scenario 3' to 5' ssDNA translocation is consistent with lack of detectable unwinding product from a 5' ssDNA tailed duplex in standard helicase assays (5,6). In the reeling reaction Hel308 could remove other DNA bound proteins during translocation like a "wire-stripper"(15), for which the domain 2 β-hairpin may help to dislodge proteins instead of DNA strands. Such activity might facilitate DNA repair by removing ssDNA binding proteins such as RPA, with which Hel308 physically interacts (12). A 'reeling' mechanism involving a secondary DNA binding site without full dissociation during translocation to remove bound proteins has been proposed for Rep, PcrA and NS3 helicases (27) but further investigation is needed to test this model in Hel308.

In the second part of this study we analyzed the effect of mutating phenylalanine residues at interface of Hel308 WHD with RecA-like domain 1. This is a common structural theme in Ski2 helicases more generally, most obviously in Brr3 and Prp3 (18,23,28,29). These mutant proteins showed drastically reduced ATPase and helicase activities. It is unclear how the WHD-RecA domain interface could control ATPase and helicase activity. Alteration of protein structure in the mutants is a possible explanation, because the mutant proteins bound to DNA with affinity reduced from wild type, but the reduced DNA binding was much less significant than the effect of these mutations on ATPase and helicase activity. It is possible that both moderately reduced DNA binding by F434 and F439 mutants, and their dramatic loss of helicase activity, is caused by the WHD being no longer orientated optimally for associating with DNA substrates, or that the stability of the protein-DNA complex formed after association is sub-optimal compared to wild type. Inter-connectivity of RecA domains 1

and 2 with the WHD in the Hel308 structures may also be disturbed by mutations in the WHD – domain 1 interface. There is some conformational movement between Hel308 RecA-like domain 2 and the WHD (30) possibly facilitated by a linker region located between RecA-like domain 2 and the WHD. The WHD may position RecA-like domains 1 and 2 correctly for cycles of ATP binding and hydrolysis required for ssDNA translocation. Although exact roles for these two invariant phenylalanine residues are unclear, effects of their mutation highlight a critical functional role for the WHD that is integrated with the core helicase domains, and with relevance for function of other Ski2 family helicases that show similar structural topology to Hel308 in this respect.

Methods

Genetic assay for *Methanothermobacter thermautotrophicus* Hel308 function

Assessment of archaeal Hel308 activity by genetic assay in *E. coli* strain *dnaE486* Δ*recQ* is described fully elsewhere (5,24). Routine growth and handling of this strain is at 30^{o}C, except for a 30 second, 42^{o}C, heat shock step during the plasmid transformation protocol. For viability "spot" tests, *E. coli* cells transformed by plasmid encoding RecQ or Hel308 protein, or an empty plasmid control, were grown as overnight cultures in Luria–Bertani medium (LB) containing ampicillin (50 μg/ml). These were used to inoculate fresh LB for growth to O.D.600 of 0.8, before serial dilution of the cultures into M9 minimal medium. Ten microliters of each dilution was spotted onto LB agar plates and the agar plates were incubated at 30^{o}C or 37^{o}C, as indicated. The strain becomes unstable for DNA replication (semi-permissive) at 37^{o} degrees, allowing the phenotype associated with expression of wild type Hel308 to be observed. In each assay a control agar plate was also incubated at 42^{o}C, which is non-permissive for growth of *dnaE486* Δ*recQ*, and from which we would expect no colony growth unless suppressor mutations or contamination had occurred.

For western blots, a 1 mL sample of each culture was taken at O.D. 0.8 and cell pellets were prepared for SDS-PAGE with a biotinylated protein size marker. The resulting gel was electro-blotted to immobilize proteins onto PVDF. This was probed with polyclonal antibodies raised against purified Mth Hel308. Antibodies had been purified against immobilized MthHel308 and against *E. coli* total cell extract, showing high specificity and sensitivity for MthHel308, detailed elsewhere (12). HRP-conjugates of an anti-biotin antibody, and a mouse anti-rabbit antibody were used to generate a signal from PVDF immobilized proteins using an enhanced chemiluminescence (ECL) kit from Pierce-Thermo-Fisher.

Cloning, expression and purification of isolated archaeal Hel308 and Human HelQ WHD proteins

Plasmids used are listed in Supplementary methods. Cloning, expression and purification of full length Hel308 from *Methanothermobacter thermautotrophicus* (Mth) was as described in (20). Amino acid sequences identified as forming WHDs of *Methanothermobacter* and human Hel308/HelQ are defined in Supplementary Table 2, predicted from alignments of Hel308 sequences for which crystal structures are available, and using Phyre2 (26). The DNA sequences encoding these WHDs were synthesized and delivered in plasmids by GeneArt (Life Technologies) with codons optimized for protein expression in *E. coli*. Coding sequences were sub-cloned from these constructs into pET14b for expression of N-terminally hexahistidine $(His)_6$ tagged WHDs. The Q5 site-directed mutagenesis system (New England Biolabs) was used to generate mutations, sequence deletions or insertions for all of the amino acid alterations to the WHD described. The *recQ* helicase gene was cloned as described in (5), for use in genetic analysis.

Mth and human WHD proteins were expressed and purified in the same way. *E. coli* strain BL21 AI was used to produce each WHD, using the method described for full length Mth Hel308 (5). The WHD proteins were insoluble when expressed under a variety of different conditions. Harvested cells were suspended in Buffer WHD (20 mM Tris. HCl pH 8.0; 2.0 M NaCl; 10 mM DTT, 1.0 % v/v Tween 20; 10% v/v glycerol) containing a protease inhibitor cocktail (SIGMAFAST^{TM}) and freeze-thawed repeatedly at -80^{o}C and room temperature prior to sonication and clarification at 58000 g in an Avanti J26-XP centrifuge. The insoluble fraction (P1) was then washed repeatedly in buffer WHD and clarified as before, giving insoluble material (P2) containing WHD protein. P2 was suspended in buffer WHD containing 6 M urea for 18 hours at 37^{o}C and clarified as before. A substantial proportion of WHD protein was present in the soluble fraction (S3) and this was dialyzed extensively into buffer A (20 mM Tris. HCl pH 8.0; 500 mM NaCl; 10% v/v glycerol) for loading a 5 mL Hi-Trap Ni-NTA column to bind to the $(His)_6$ tag of each protein. WHD proteins were eluted in buffer WHD, in an imidazole concentration gradient of 0.005-200 mM. WHD containing fractions were dialyzed into buffer B (20 mM Tris. HCl pH 8.0, 100 mM NaCl, 10% v/v glycerol and 5 mM DTT) and loaded into a 1 mL Hi-Trap heparin column. Purified WHD proteins eluted from heparin at 300-500 mM NaCl and were then dialyzed into buffer B containing 40 % v/v glycerol, for storage in aliquots at -80^{o}C. Protein concentrations were estimated in two measurements using Bradford's reagent in kit form from Bio-Rad. First to determine wild type Hel308 and WHD protein concentration against a standard curve of bovine serum albumin protein concentrations, and second by using wild type Hel308/HelQ protein concentration to generate a standard curve for determination of relative concentrations of mutant Hel308 and WHD proteins. Purified WHD proteins were assessed for re-folding into a single species by size exclusion chromatography through a superose-12 column.

EMSAs, ATPase and helicase unwinding assays

Structures and sequences of DNA substrates used in EMSAs and helicase assays are given in the Supplementary material. In each case DNA was 5'-end labeled with γ ^{32}P from ^{32}P-ATP using T4 polynucleotide kinase. EMSAs followed standard procedures with protein-DNA binding at ambient temperature for 10 minutes initially prior to loading reactions onto a 5% w/v acrylamide Tris-Borate-EDTA (TBE) gel for electrophoresis at 150 volts in protean II systems (Bio-Rad) for 1.5 - 2 hours. Reactions mixed Hel308 or HelQ proteins, typically in the range 0 – 250 nM, with 6 nM of ^{32}P end labeled DNA (unless stated otherwise) in buffer HB (20 mM Tris. HCL pH 7.5. 100 ug/mL BSA, 8% v/v glycerol, 1 mM DTT).

ATPase assays used the malachite green reporter method (31) that measures liberation of phosphate from ATP by absorbance at 660 nm, and in these assays used single stranded DNA (supplementary materials) to stimulate Hel308 activity. Helicase unwinding assays for Hel308 were in buffer HB supplemented with 5 mM ATP and 5 mM magnesium chloride at 43^{o}C, for either 5 minutes or as a function of time, as stated. Reactions were stopped by addition of 10 uL of 4 mg/mL proteinase K and 1% w/v SDS and loaded onto a 10% w/v acrylamide TBE gel in bromophenol blue/xylene cyanol loading dye. Gels containing radiolabelled DNA were dried on a heated vacuum drier and developed using phosphorimaging screens, which were exposed on a FujiFilm FLA3000 machine. This generated TIFF images for analysis and quantification using GIMP, Adobe Photoshop and GelEval FrogDance software.

Fluorescence anisotropy

The binding affinity of Hel308 WT, Hel308 Y460A and Hel308 QYN mutants was investigated by fluorescence anisotropy using a Cary Eclipse fluorescence spectrophotometer (Varian) equipped with automatic polarizers as previously described (32). All experiments were carried out at room temperature. The fork-2 substrate was constructed from two strands (Integrated DNA Technologies), one of them carrying a 6-(carboxyfluorescein) dye (FAM) at the 5' end (5'-FAM-GTCGGATCCTCTAGACAGCTCCATGATCACTGGCACTGGTAGAATTCGGC). This strand was hybridized to a partially complementary oligonucleotide sequence (5'-CAACGTCATAGACGATTACATTGCTACATGGAGCTGTCTAGAGGATCCGA) by heating to 90°C for 2 min followed by slow cooling overnight. The hybridized construct was purified by 10% polyacrylamide gel electrophoresis followed by ethanol precipitation. Fork-2 substrate was re-suspended in anisotropy buffer (50 mM Tris-HCl, pH 7.5) and quantified by absorption spectrophotometry. The FAM-labeled Fork-2 substrate was used at a final

concentration of 10 nM in 150 μl of anisotropy buffer. The protein concentration was increased cumulatively with corrections made for dilution. Anisotropy values were collected in quadruplicate with excitation at 490 nm and emission at 520 nm, corresponding to the absorption and emission maxima of the FAM dye. Data were analyzed using Origin 2017 (OriginLab Corporation, USA) and fitted to the following quadratic equation, $A = A_{min} + [(D+E+K_D)-\{(D+E+K_D)^2-(4DE)\}^{1/2}](A_{max}-A_{min})/(2D)$, where A is the measured anisotropy, E is the total protein concentration, and D represents the total DNA concentration. A_{max} and A_{min} represent the maximum and minimum anisotropy values at saturating protein concentration and in absence of protein, respectively. The titration curves were fitted assuming a 1:1 interaction between the protein and the DNA.

Analytical gel filtration of WHD proteins

Analytical size exclusion chromatography was carried out using a superpose-12 column to assess purified WHD proteins in 20 mM Tris pH 8.0 containing 150 mM NaCl (Figure S4). Traces for elution of WHD protein were compared to that of a gel filtration size standard (Bio-Rad, product 151-1901), shown in supplementary data.

Acknowledgements

Research in PS and ELB laboratories is supported by BBSRC grants BB/K021540/1 and BB/M020541/1. SJN was funded by a University of Nottingham PhD studentship. We thank Laura Kirkham for help with genetic analysis.

Conflict of Interest Statement

The authors declare that there is no conflict of interest in publication of this paper.

References

1. Marini, F. and Wood, R.D. (2002) A human DNA helicase homologous to the DNA cross-link sensitivity protein Mus308. *The Journal of Biological Chemistry*, **277**, 8716-8723.
2. Muzzini, D.M., Plevani, P., Boulton, S.J., Cassata, G. and Marini, F. (2008) Caenorhabditis elegans POLQ-1 and HEL-308 function in two distinct DNA interstrand cross-link repair pathways. *DNA Repair*, **7**, 941-950.
3. Ward, J.D., Muzzini, D.M., Petalcorin, M.I., Martinez-Perez, E., Martin, J.S., Plevani, P., Cassata, G., Marini, F. and Boulton, S.J. (2010) Overlapping mechanisms promote postsynaptic RAD-51 filament disassembly during meiotic double-strand break repair. *Molecular Cell*, **37**, 259-272.
4. Laurencon, A., Orme, C.M., Peters, H.K., Boulton, C.L., Vladar, E.K., Langley, S.A., Bakis, E.P., Harris, D.T., Harris, N.J., Wayson, S.M. *et al.* (2004) A large-scale screen for mutagen-sensitive loci in Drosophila. *Genetics*, **167**, 217-231.
5. Guy, C.P. and Bolt, E.L. (2005) Archaeal Hel308 helicase targets replication forks in vivo and in vitro and unwinds lagging strands. *Nucleic Acids Research*, **33**, 3678-3690.
6. Fujikane, R., Komori, K., Shinagawa, H. and Ishino, Y. (2005) Identification of a Novel Helicase Activity Unwinding Branched DNAs from the Hyperthermophilic Archaeon, Pyrococcus furiosus. *The Journal of Biological Chemistry*, **280**, 12351-12358.
7. Luebben, S.W., Kawabata, T., Akre, M.K., Lee, W.L., Johnson, C.S., O'Sullivan, M.G. and Shima, N. (2013) Helq acts in parallel to Fancc to suppress replication-associated genome instability. *Nucleic Acids Research*, **41**, 10283-10297.
8. Tafel, A.A., Wu, L. and McHugh, P.J. (2011) Human HEL308 localizes to damaged replication forks and unwinds lagging strand structures. *The Journal of Biological Chemistry*, **286**, 15832-15840.
9. Northall, S.J., Ivancic-Bace, I., Soultanas, P. and Bolt, E.L. (2016) Remodeling and Control of Homologous Recombination by DNA Helicases and Translocases that Target Recombinases and Synapsis. *Genes*, **7**.
10. Adelman, C.A., Lolo, R.L., Birkbak, N.J., Murina, O., Matsuzaki, K., Horejsi, Z., Parmar, K., Borel, V., Skehel, J.M., Stamp, G. *et al.* (2013) HELQ promotes RAD51 paralogue-dependent repair to avert germ cell loss and tumorigenesis. *Nature*, **502**, 381-384.
11. Takata, K., Reh, S., Tomida, J., Person, M.D. and Wood, R.D. (2013) Human DNA helicase HELQ participates in DNA interstrand crosslink tolerance with ATR and RAD51 paralogs. *Nature Communications*, **4**, 2338.
12. Woodman, I.L., Brammer, K. and Bolt, E.L. (2011) Physical interaction between archaeal DNA repair helicase Hel308 and Replication Protein A (RPA). *DNA Repair*, **10**, 306-313.
13. Hong, Y., Chu, M., Li, Y., Ni, J., Sheng, D., Hou, G., She, Q. and Shen, Y. (2012) Dissection of the functional domains of an archaeal Holliday junction helicase. *DNA Repair*, **11**, 102-111.
14. Li, Z., Lu, S., Hou, G., Ma, X., Sheng, D., Ni, J. and Shen, Y. (2008) Hjm/Hel308A DNA helicase from Sulfolobus tokodaii promotes replication fork regression and interacts with Hjc endonuclease in vitro. *Journal of Bacteriology*, **190**, 3006-3017.

15. Richards, J.D., Johnson, K.A., Liu, H., McRobbie, A.M., McMahon, S., Oke, M., Carter, L., Naismith, J.H. and White, M.F. (2008) Structure of the DNA repair helicase hel308 reveals DNA binding and autoinhibitory domains. *The Journal of Biological Chemistry*, **283**, 5118-5126.
16. Buttner, K., Nehring, S. and Hopfner, K.P. (2007) Structural basis for DNA duplex separation by a superfamily-2 helicase. *Nature Structural & Molecular Biology*, **14**, 647-652.
17. Oyama, T., Oka, H., Mayanagi, K., Shirai, T., Matoba, K., Fujikane, R., Ishino, Y. and Morikawa, K. (2009) Atomic structures and functional implications of the archaeal RecQ-like helicase Hjm. *BMC Structural Biology*, **9**, 2.
18. Johnson, S.J. and Jackson, R.N. (2013) Ski2-like RNA helicase structures: common themes and complex assemblies. *RNA Biology*, **10**, 33-43.
19. Derrington, I.M., Craig, J.M., Stava, E., Laszlo, A.H., Ross, B.C., Brinkerhoff, H., Nova, I.C., Doering, K., Tickman, B.I., Ronaghi, M. *et al.* (2015) Subangstrom single-molecule measurements of motor proteins using a nanopore. *Nature Biotechnology*, **33**, 1073-1075.
20. Woodman, I.L., Briggs, G.S. and Bolt, E.L. (2007) Archaeal Hel308 domain V couples DNA binding to ATP hydrolysis and positions DNA for unwinding over the helicase ratchet. *J Mol Biol*, **374**, 1139-1144.
21. Harami, G.M., Gyimesi, M. and Kovacs, M. (2013) From keys to bulldozers: expanding roles for winged helix domains in nucleic-acid-binding proteins. *Trends in Biochemical Sciences*, **38**, 364-371.
22. Fujikane, R., Shinagawa, H. and Ishino, Y. (2006) The archaeal Hjm helicase has recQ-like functions, and may be involved in repair of stalled replication fork. *Genes to Cells*, **11**, 99-110.
23. Woodman, I.L. and Bolt, E.L. (2011) Winged helix domains with unknown function in Hel308 and related helicases. *Biochemical Society Transactions*, **39**, 140-144.
24. Hishida, T., Han, Y.W., Shibata, T., Kubota, Y., Ishino, Y., Iwasaki, H. and Shinagawa, H. (2004) Role of the Escherichia coli RecQ DNA helicase in SOS signaling and genome stabilization at stalled replication forks. *Genes & Development*, **18**, 1886-1897.
25. Wechsler, J.A. and Gross, J.D. (1971) Escherichia coli mutants temperature-sensitive for DNA synthesis. *Mol Gen Genet*, **113**, 273-284.
26. Kelley, L.A., Mezulis, S., Yates, C.M., Wass, M.N. and Sternberg, M.J. (2015) The Phyre2 web portal for protein modeling, prediction and analysis. *Nature Protocols*, **10**, 845-858.
27. Lin, C.T., Tritschler, F., Lee, K.S., Gu, M., Rice, C.M. and Ha, T. (2017) Single-molecule imaging reveals the translocation and DNA looping dynamics of hepatitis C virus NS3 helicase. *Protein Science : a publication of the Protein Society*.
28. Pena, V., Jovin, S.M., Fabrizio, P., Orlowski, J., Bujnicki, J.M., Luhrmann, R. and Wahl, M.C. (2009) Common design principles in the spliceosomal RNA helicase Brr2 and in the Hel308 DNA helicase. *Molecular Cell*, **35**, 454-466.
29. Zhang, L., Xu, T., Maeder, C., Bud, L.O., Shanks, J., Nix, J., Guthrie, C., Pleiss, J.A. and Zhao, R. (2009) Structural evidence for consecutive Hel308-like modules in the spliceosomal ATPase Brr2. *Nature Structural & Molecular Biology*, **16**, 731-739.
30. Flechsig, H., Popp, D. and Mikhailov, A.S. (2011) In silico investigation of conformational motions in superfamily 2 helicase proteins. *PloS one*, **6**, e21809.
31. Bird, L.E., Hakansson, K., Pan, H. and Wigley, D.B. (1997) Characterization and crystallization of the helicase domain of bacteriophage T7 gene 4 protein. *Nucleic Acids Research*, **25**, 2620-2626.
32. Constantinescu-Aruxandei, D., Petrovic-Stojanovska, B., Penedo, J.C., White, M.F. and Naismith, J.H. (2016) Mechanism of DNA loading by the DNA repair helicase XPD. *Nucleic Acids Research*, **44**, 2806-2815.

Figure 1.

(A). The atomic resolution structure of archaeal Hel308 from *Archaeoglobus fulgidus* (Afu), bound to a minimal helicase substrate (3' ssDNA tailed duplex, orange), from PDB ID 2P6R (16). The structure is orientated to give a clear view of the winged helix domain 3 (WHD) highlighted in blue. Bound DNA is in orange, and core helicase domains 1, 2 and 4 are in grey (labeled d1, d2 and d5), except for part of RecA-like domain 1 that is highlighted in green where it forms an interface with the WHD. Detail of the WHD is given boxed, highlighting the positions of tyrosine and phenylalanine residues described in this work.

(B). Alignment of WHD amino acids from the three crystal structures of archaeal Hel308 (*Sulfolobus solfataricus*, Sso; *Pyroccocus furiosus*, Pfu and *Archaeoglobus fulgidus*, Afu) plus *Methanothermobacter thermautotrophicus,* Mth, the Hel308 enzyme that was used in this study. Amino acid numbering shown is derived from Mth Hel308. Highlighted are the solvent exposed α-helix (α-20) targeted for mutagenesis containing a well-conserved tyrosine residue, and the conserved phenylalanine residues (F434 and F439) from the "inward" face of the WHD that packs against a RecA-like helicase domain.

Figure 2.

(A). Graph summarizing data from a genetic assay for activity of Hel308 mutants with amino acid substitutions in WHD α-20. Details of the *E. coli* strain used (*dnaE486* Δ*recQ*) are in the main text. Plasmid expression of RecQ or wild type Hel308 ("wild type") was toxic, causing low cell viability that is the standard measure of Hel308 function (shown with *). Cells expressing Hel308^{Y460A} (Y460A) or Hel308^{QYN} (QYN) at 37^{o}C showed improved viability that was intermediate to viability of cells expressing ATPase defective Hel308^{K51L} (K51L) or cells containing empty plasmid (Empty).

(B). Western blot detection of MthHel308 using purified polyclonal anti-Hel308 antibodies. See also supplementary Figure S4, showing the entire gel. Hel308^{WT} and mutant proteins Hel308^{QYN} , Hel308^{Y460A} , and Hel308^{K51L} were all expressed detectably in *E. coli dnaE486* Δ*recQ* cells, as indicated alongside cells lacking Hel308 expression (pEmpty). The marker was a Biotinylated protein ladder from Cell Signalling, which includes an 80 kDa marker band closely corresponding to the size of Hel308 at 75 kDa.

Figure 3.

(A). Helicase activity of Hel308^{Y460A} and Hel308^{QYN} compared to wild type Hel308. Graphs show unwinding activity as a function of time for each protein mixed with DNA fork-2 or 3' ssDNA tailed duplex, as indicated, with DNA strand lengths (nucleotides) indicated next to

each substrate. In each case protein (100 nM) was mixed with 5' end-radiolabelled (*) DNA substrate (10 nM). Samples of the reaction mixture were taken at the following time points (in seconds), as indicated in the graphs; 0, 30, 60, 90, 120, 150 and 180, except for 3' tailed duplex which lacked a 180 s sample. Assays were done three times; error bars represent standard deviation from the mean, calculated using GraphPad Prism software. Gel panels give one example gel for each Hel308/Hel308^{QYN} unwinding assay that was quantified, with substrate and product DNA molecules indicated. **(B).** Binding affinities of wild-type Hel308 (left panel), Hel308^{Y60A} (middle panel) and Hel308^{QYN} (right panel) were measured using a fluorescence anisotropy assay. Increasing concentrations of a particular protein were added to a solution containing a fork-2 substrate labeled at the 5' duplex end with a 6-carboxyfluorescein (FAM) reporter. Protein binding to the DNA leads to an increase in the anisotropy value from which dissociation constant can be calculated. The means of quadruplicate measurements were plotted and the standard errors are also shown. Each binding isotherm was fitted to a 1:1 binding model using a quadratic equation (see materials section) to extract the dissociation constant. This binding model was used based on observation of a single protein-fork2 complex in EMSAs when Hel308 was used at <200 nM, corresponding to concentrations of Hel308 that gave the major binding curve data during anisotropy. Standard errors derived from the curve fitting are also shown.

Figure 4

(A). EMSAs showing DNA binding by isolated WHD protein from archaeal Hel308. Purified wild type WHD protein (WHD^{WT}) bound duplex DNA (lanes 1-5), but binding was lost from WHD^{QYN}, lanes 6-9). Radiolabelled duplex DNA (10 nM, *) was incubated with WHD proteins at 0, 25, 50, 100 and 200 nM, as indicated. WHD^{WT} did not bind to the equivalent ssDNA (lanes 10-13), shown in comparison to ssDNA binding by full length Hel308 (lanes 14 and 15). Reactions contained 6 nM of radiolabelled (*) ssDNA substrate, and WHD^{WT} at 0, 50, 100 and 200 nM, or Hel308 at 100 and 200 nM. **(B).** The isolated HelQ WHD protein purified from *E. coli* bound radiolabelled duplex DNA (6 nM) at 5, 10 and 20 nM protein (lanes 1-4), but binding was abolished by mutation of amino acid residue pairs Y818 and K819 (Q-WHD^{YK}, lanes 5-10), at protein concentrations up to 100 nM (0, 5, 10, 20, 50 and 100 nM).

Figure 5.

(A). Graph showing data from a genetic assay for activity of Hel308 mutants with amino acid substitutions in F434 or F439 at the interface of WHD and RecA-like domain 1. Plasmid expression of wild type Hel308 (pHel308^{WT}) was toxic causing low cell viability that is the standard measure of Hel308 function (shown with *). Cells expressing Hel308 mutated in either phenylalanine residue showed much improved viabilities, phenotypes more similar to

K51L or empty plasmid and consistent with much reduced Hel308 activity. **(B).** Reduced ATPase activity of F434V and F439A Hel308 proteins measured in malachite green reporter assays, detecting liberation of phosphate from ATP. Assays were in duplicate, error bars recording standard deviation calculated using Prism software. Reactions contained 100 nM of protein in the presence of 5 mM ATP and 5 mM magnesium chloride, supplemented with 1 μg of ssDNA oligonucleotide to stimulate Hel308 ATPase activity. **(C).** Helicase activities of F434V and F439A Hel308 proteins compared to wild type protein. The graph shows mean unwinding activity of the two mutant proteins compared to wild type protein when 100 nM of protein was mixed with 6 nM of fork-2 DNA in the presence of ATP and magnesium, measured as a function of time. The graph plots mean values for unwinding, from reactions repeated three times, with error bars representing the standard deviation from the mean. Representative gels used for the graph are also shown.

Figure 6. Models for Hel308 helicase mechanism either **(A)** unwinding a 3' tailed partial duplex by translocation 3' to 5' along ssDNA or **(B)** ssDNA "reeling" in a 5' tailed partial duplex by 3' to 5' translocation, but without observable helicase unwinding of this substrate. In the latter, the role of Hel308 may be to remove other bound proteins from ssDNA, shown as yellow circles. The β-hairpin located in domain 2 could be crucial to both DNA strand separation during helicase activity, and for removal of proteins during a "reeling" reaction. In each model core helicase domains 1, 2 and 4 bind to ssDNA as in the crystal structure of archaeal Hel308 (Figure 1 and [16]) triggering ATPase activity and translocation. The winged helix domain binds to duplex DNA to assist with the efficacy of helicase/translocase activity and act as a platform to orientate the core domains for translocation.

1A

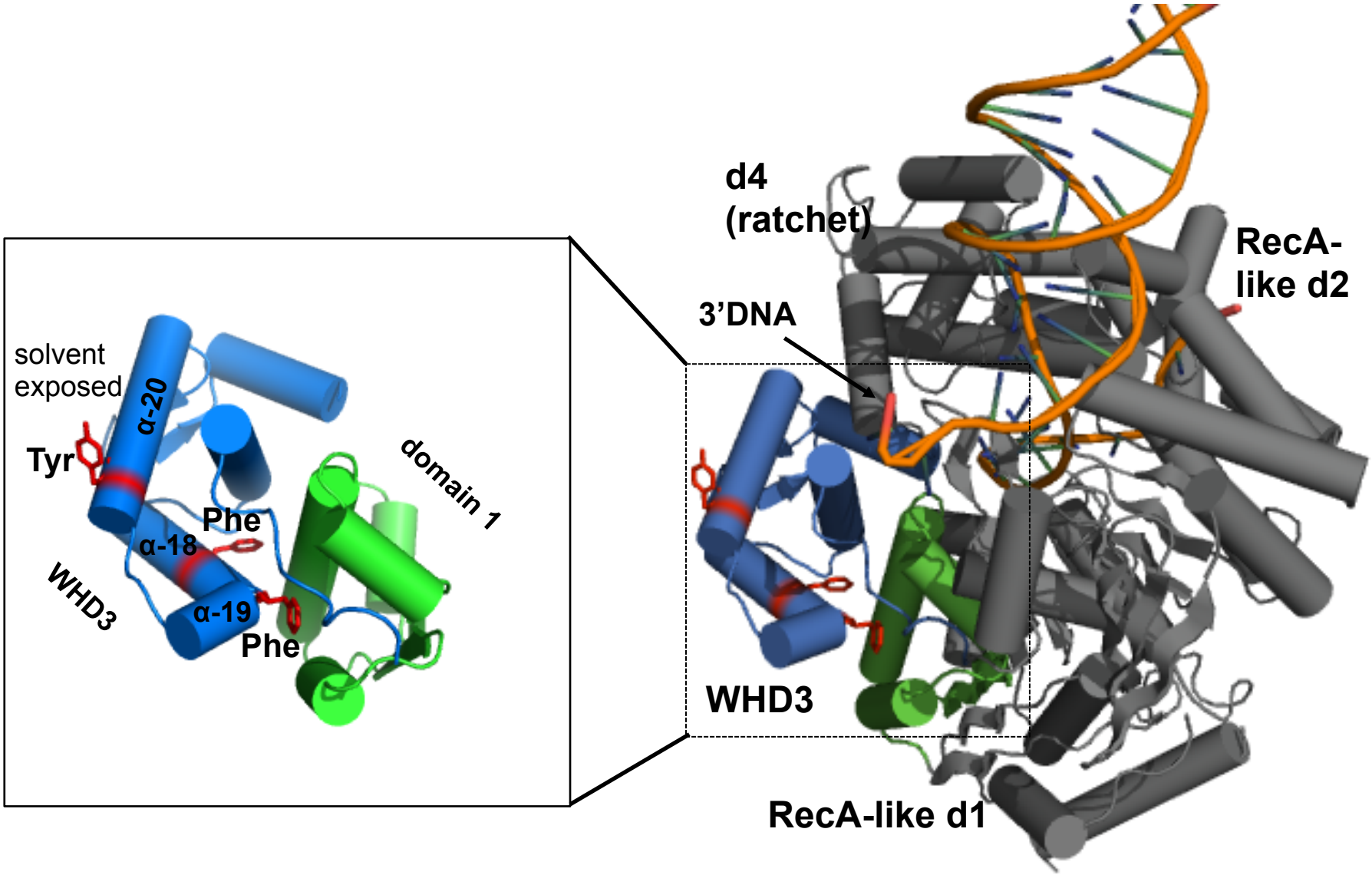
solvent
exposed
α-20
Tyr
Phe
α-18
WHD3
α-19
Phe
domain 1
d4
(ratchet)
3'DNA
RecA-
like d2
WHD3
RecA-like d1

1B

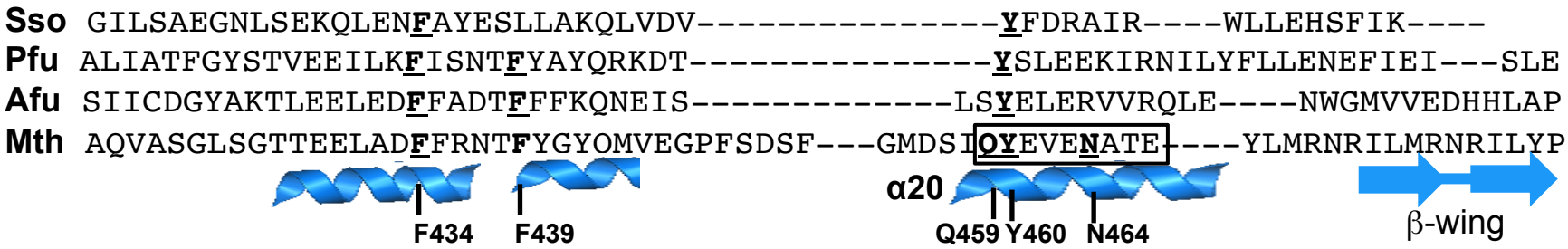
Sso GILSAEGNLSEKQLENFAYESLLAKQLVDV----------YFDRAIR----WLLEHSFIK----
Pfu ALIATFGYSTVEEILKFISNTFYAYQRKDT----------YSLEEKIRNILYFLLENEFIEI---SLE
Afu SIICDGYAKTLEELEDFFADTFFFKQNEIS----------LSYELERVVRQLE----NWGMVVEDHHLAP
Mth AQVASGLSGTTEELADFFRNTFYGYQMVEGPFSDSF---GMDSIQYEVENATE----YLMRNRILMRNRILYP
F434
F439
α20
Q459
Y460
N464
β-wing

2

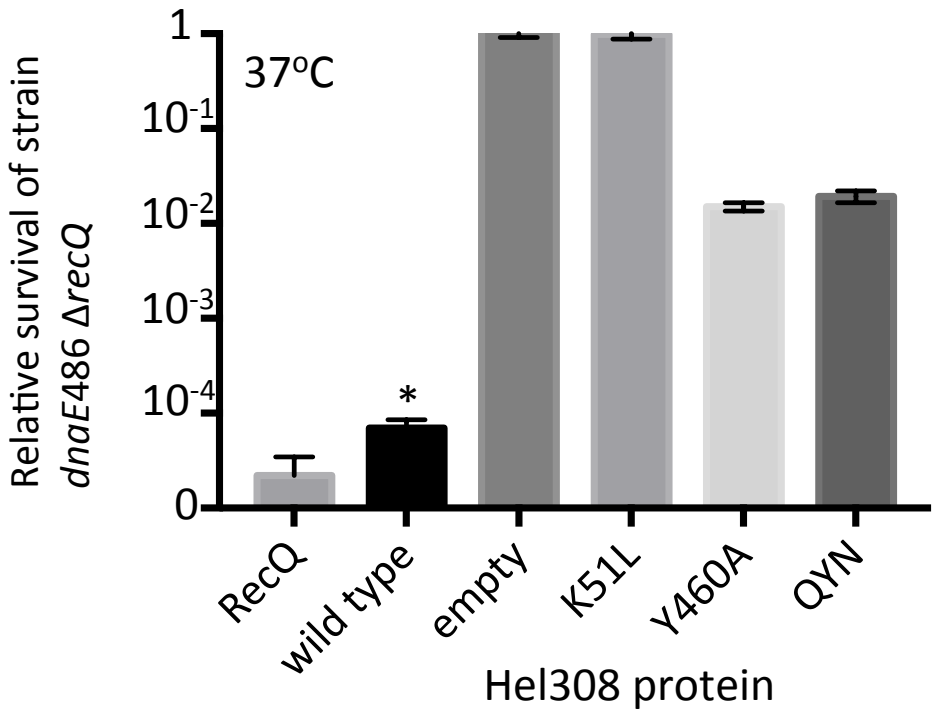
Relative survival of strain
dnaE486 ΔrecQ
37°C
1
10-1
10-2
10-3
10-4
0
*
RecQ
wild type
empty
K51L
Y460A
QYN
Hel308 protein

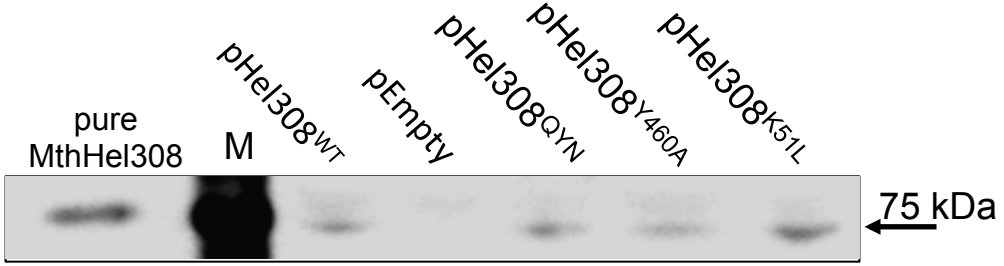
pure MthHel308
M
pHel308WT
pEmpty
pHel308QYN
pHel308Y460A
pHel308K51L
75 kDa

3A

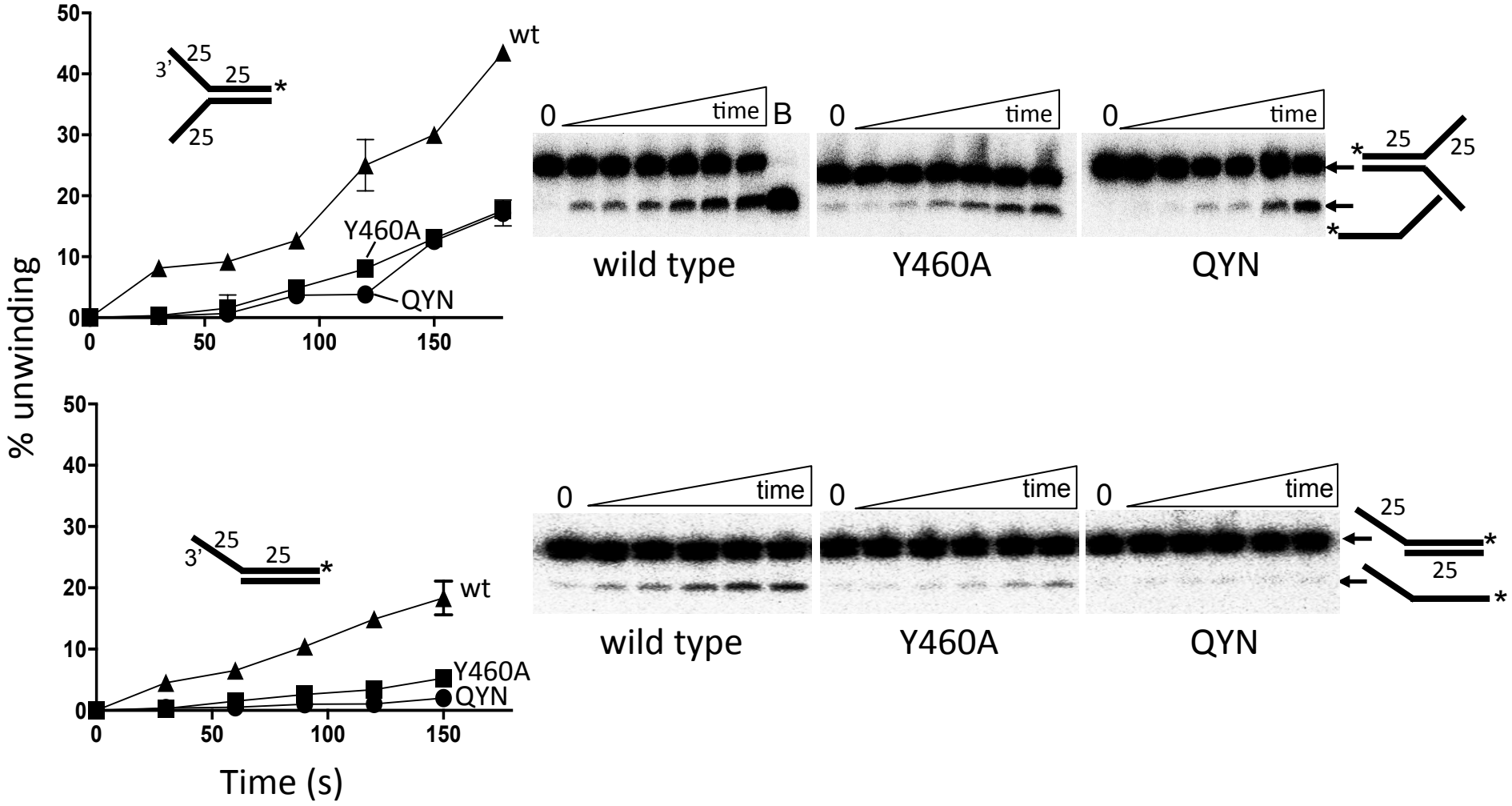
% unwinding
Time (s)
wt
Y460A
QYN
3'
25
25
*
0
time
B
wild type
Y460A
QYN

3B

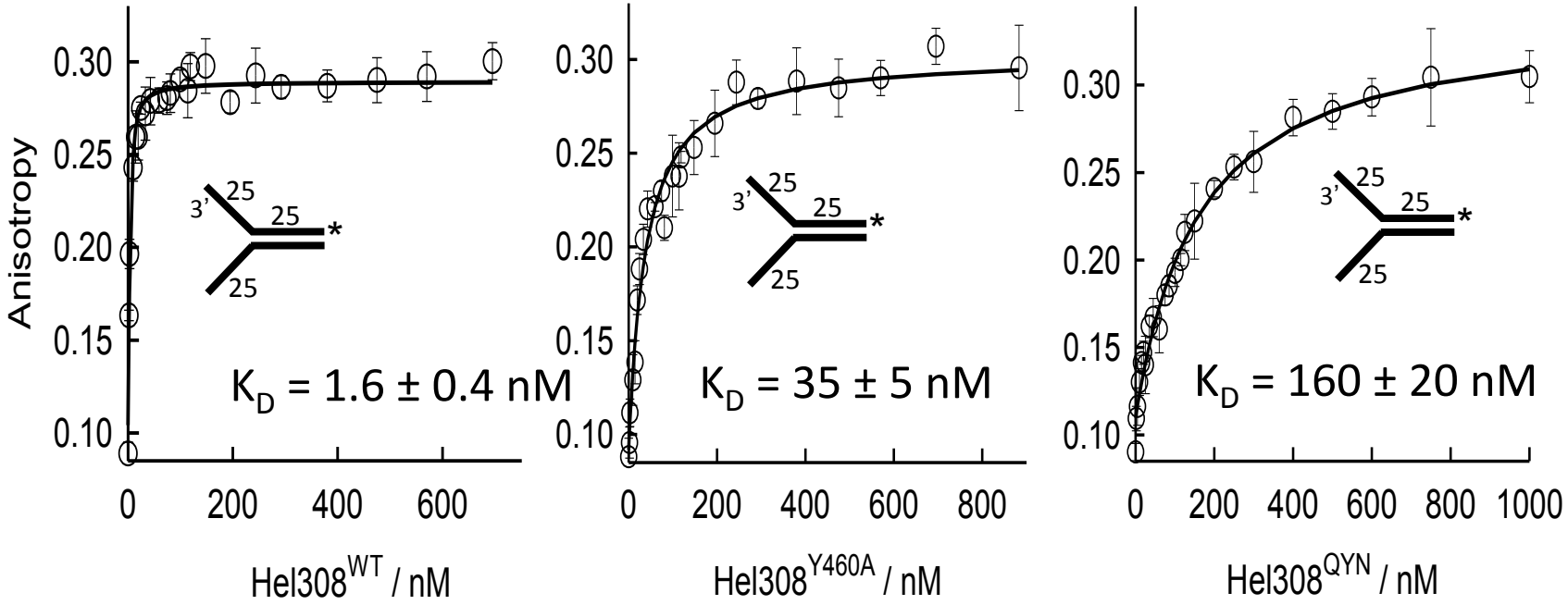
Anisotropy
0.30
0.25
0.20
0.15
0.10
0
200
400
600
800
1000
3'
25
25
25
*
K_D = 1.6 ± 0.4 nM
K_D = 35 ± 5 nM
K_D = 160 ± 20 nM
Hel308^{WT} / nM
Hel308^{Y460A} / nM
Hel308^{QYN} / nM

4A

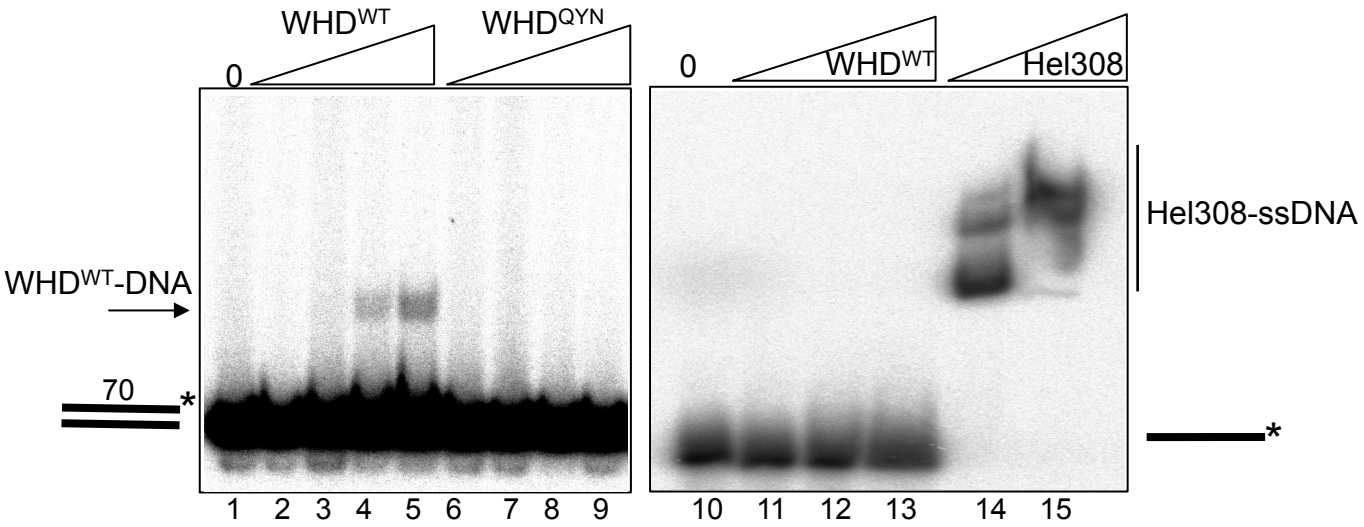
WHD^WT
WHD^QYN
0
0
WHD^WT
Hel308
WHD^WT-DNA
70
*
Hel308-ssDNA
*
1 2 3 4 5 6 7 8 9
10 11 12 13 14 15

4B

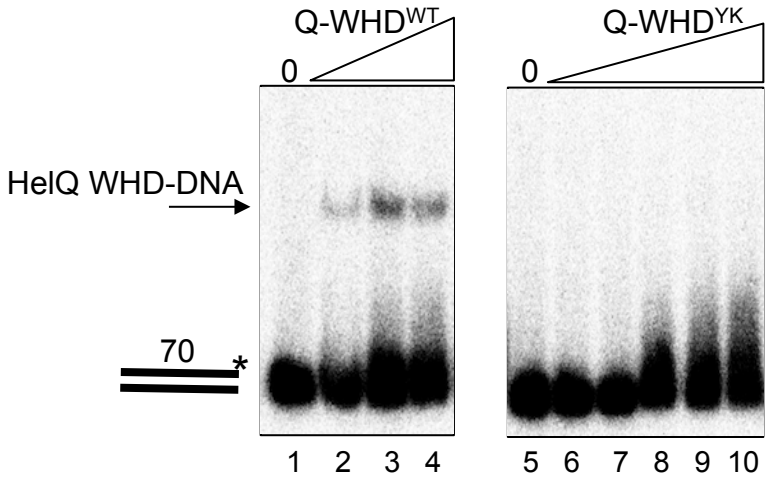
Q-WHD^WT
Q-WHD^YK
0
0
HelQ WHD-DNA
70
*
1 2 3 4
5 6 7 8 9 10

5A

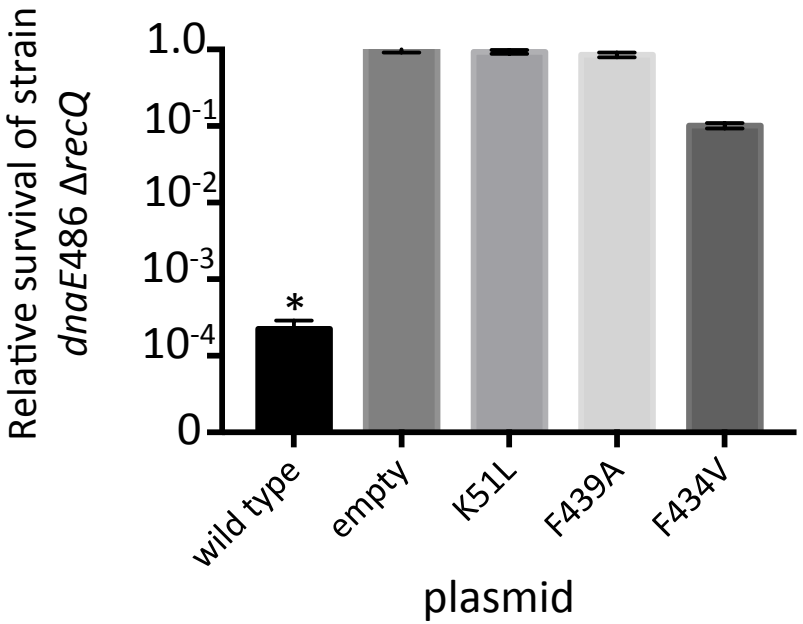
Relative survival of strain
dnaE486 ΔrecQ
1.0
10-1
10-2
10-3
10-4
0
*
wild type
empty
K51L
F439A
F434V
plasmid

5B

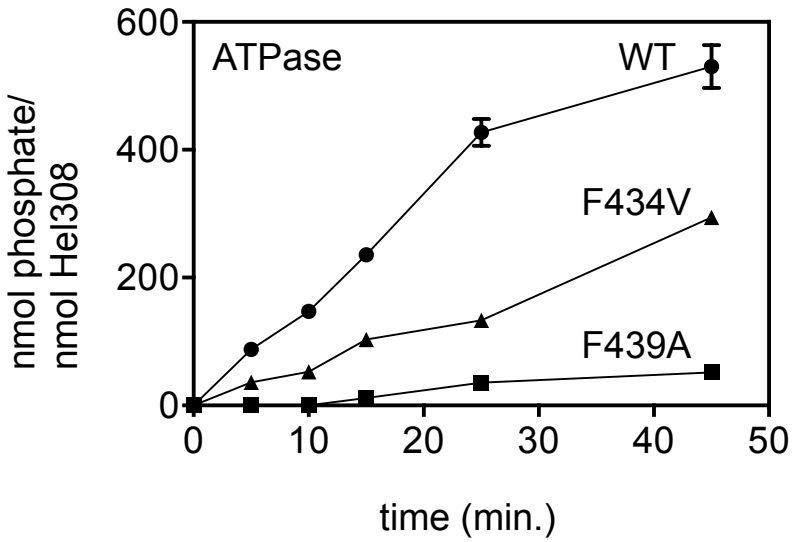
600
400
200
0
ATPase
WT
F434V
F439A
nmol phosphate/
nmol Hel308
0
10
20
30
40
50
time (min.)

5C

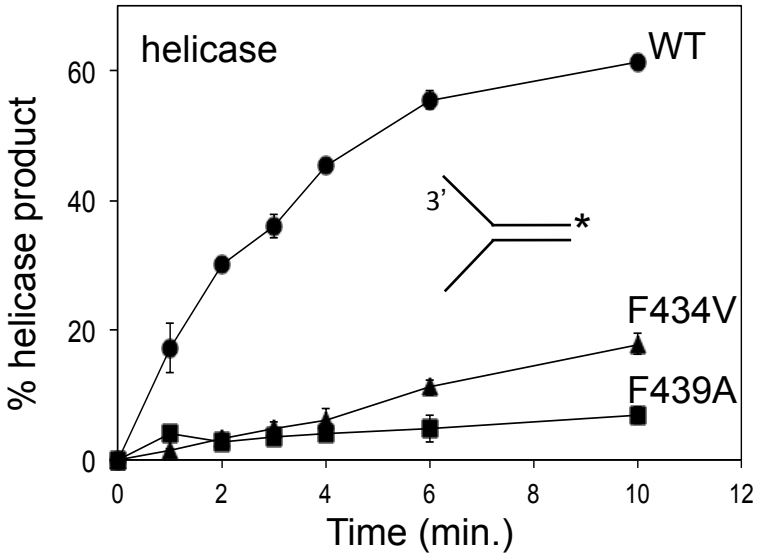
helicase
WT
F434V
F439A
3'
*
% helicase product
Time (min.)
0
20
40
60
0
2
4
6
8
10
12

6

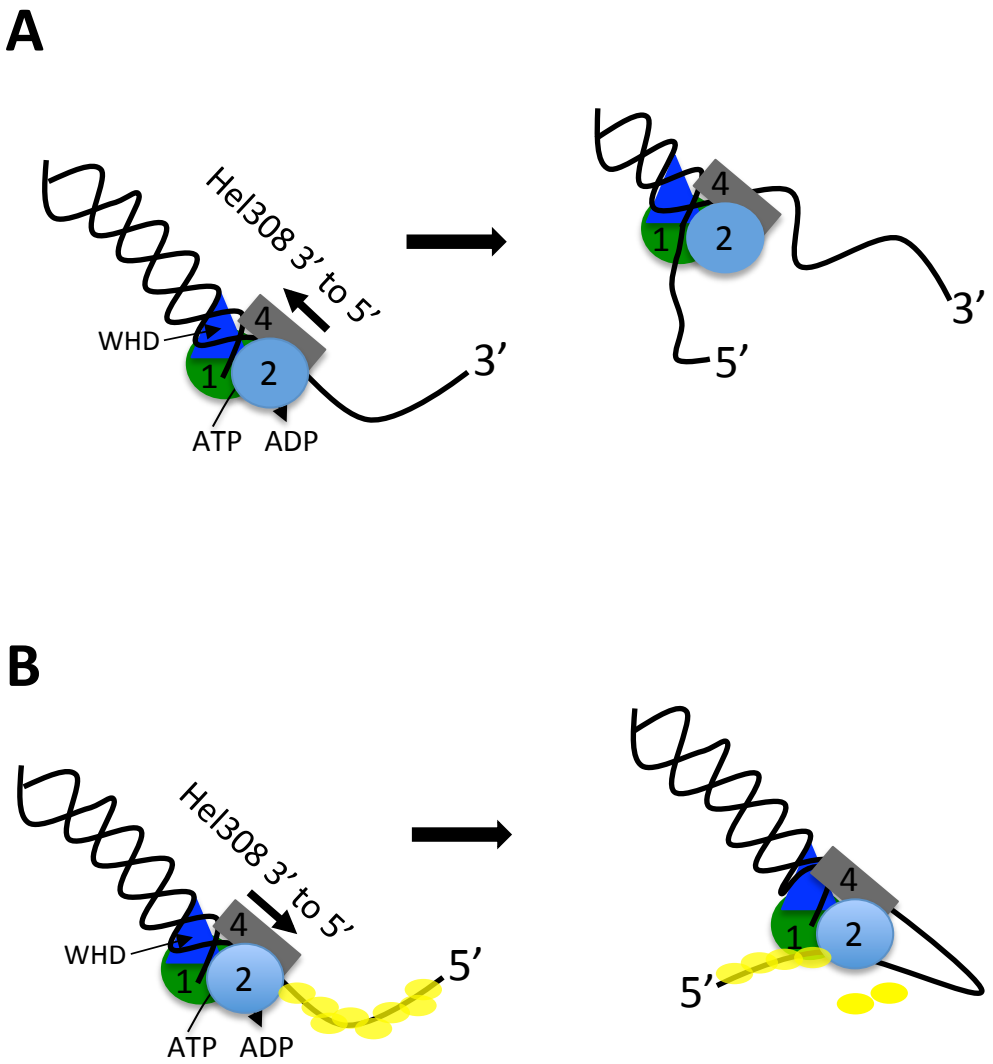
A
Hel308 3′ to 5′
WHD
4
1
2
3′
ATP
ADP
5′
B
Hel308 3′ to 5′
WHD
4
1
2
5′
ATP
ADP
5′

Supplementary Figure Legends

Figure S1. See also Figures 1A and 1B. Clustal omega alignments of amino acid sequences from archaeal Hel308 enzymes from the genera indicated. Also included is the sequence of a human Hel308 homologue, called HelQ. The first approximately 300 amino acids of human HelQ are omitted from the alignment because they give no sequence homology to any other protein. Amino acid sequences corresponding to the WHD are highlighted by a black box, within which a red box indicates the solvent-exposed α-helix (α-20) referred to in the main results.

Figure S2.

Solved structures of Hel308 from *Pyrococcus furiosus* (Pfu, PDB ID 2ZJ2, (17)) and *Sulfolobus solfataricus* (Sso, PDB ID 2VA8, (15)), and a model of MthHel308 generated from Phyre2. In each of these structures highlighted in blue is the position of WHD α-20 and its tyrosine residue, referred to in the main results. The position of the C-terminal domain five is also marked (d5) to help orientate each protein molecule in the absence of bound DNA. Note that SsoHel308 crystallized as a dimer, but only one monomer is shown for clarity. At the bottom of the figure are details of the WHD topologies for the same Hel308 enzymes highlighting the relative positions of the solvent exposed α-20 tyrosine and buried phenylalanine residues, or a phenylalanine and leucine for Sso Hel308.

Figure S3.

Summary of viability "spot" tests of *E. coli* strain *dnaE*486 Δ *recQ* expressing from a plasmid either Hel308 (pHel308), *E. coli* RecQ (pRecQ) or Hel308 winged helix domain mutants (pHel308^{Y460A} or pHel308^{QYN}), assayed as described in main text and in Figure 2. Cultures of each were grown to O.D. 0.4 at permissive temperature (30^{o}C) and then immediately diluted incrementally by 10 – fold for "spotting" onto LB agar containing ampicillin and incubated at semi-permissive temperature (37^{o}C) to observe the viability phenotypes after incubation for 12-24 hours.

Figure S4.

See also Figure 2. Shown is the full gel western blot for Hel308 protein expression during the genetic assay in *E. coli* strain *dnaE*486 Δ *recQ*. The blot section shown in

Figure 2 is indicated. The identity of protein bands observed at about 40 kDa is unknown, but they are present in all lanes, including the empty plasmid that lacks Hel308. It is likely to be forms of an *E. coli* protein with cross-reactivity to the purified anti-Hel308 antibody used.

Figure S5.

Coomassie stained 8% w/v acrylamide SDS-PAGE gels showing 2 µg samples of each purified full length MthHel308 protein that was assayed in this work.

Figure S6.

(A). EMSA through a 5% acrylamide TBE gel of Hel308^{Y460A} and Hel308^{WT} binding to fork-2 DNA. Protein was used at 0, 25, 50, 100 and 200 nM and fork-2 at 10 nM. The two protein-DNA complexes typical of hel308 binding to fork-2 are indicated, formed by wild type and mutant proteins. (B). Graph showing relative ATP hydrolysis by Hel308^{Y460A} and Hel308^{QYN} compared to wild type Hel308. Assays used the malachite green reporter assay as detailed in the methods, and show mean ATPase activity from two independent experiments using the wild type Hel308 activity as a base-line control.

Figure S7.

Hel308 and human HelQ highlighting positions of WHDs that were used for cloning the isolated WHD in each case. See also Figure S1 for an amino acid sequence alignment of the same WHDs. Supplementary Table S2 gives amino acid sequences for each WHD protein. Below the cartoon are 15% w/v acrylamide SDS-PAGE gels of Coomassie blue stained purified MthHel308 WHD proteins, and human HelQ WHD proteins. Lanes for Hel308^{WT} and Hel308^{QYN} are from the same SDS-PAGE gel but have been edited together to remove an intervening lane that is not relevant to this work.

Figure S8. Elution traces for MthHel308 WHD^{WT} and WHD^{QYN} proteins from analytical size exclusion analysis through a superpose-12 column. Peak positions for the molecular weight standards are shown after super-imposing their trace over traces for the WHD proteins.

Figure S9.

EMSA of purified Hel308 WHD binding to 50 base pair and 33 base pair DNA duplexes of differing sequence. Sequences of the DNA duplexes used here and for Figures 3A and 4B are given in the supplementary information below. Duplexes were radiolabelled (6nM, *) and mixed with WHD protein at 0, 20, 40, 80, 160 and 320 nM.

Figure S10.

Summary of viability "spot" tests of *E. coli* strain *dnaE*486 Δ*recQ* expressing from a plasmid either Hel308 (pHel308), *E. coli* RecQ (pRecQ) or Hel308 winged helix domain mutants ($pHel308^{F434V}$ or $pHel308^{F439A}$), assayed as described in main text and in Figure 2. Cultures of each were grown to O.D. 0.4 at permissive temperature ($30^{o}C$) and then immediately diluted incrementally by 10 – fold for "spotting" onto LB agar containing ampicillin and incubated at semi-permissive temperature ($37^{o}C$) to observe the viability phenotypes after incubation for 12-24 hours.

Figure S11. Graph measuring binding of a DNA fork by Hel308 mutant protein F439A, the least active of all of the WHD proteins studied in this work, compared to wild type protein, for comparison with total loss of fork unwinding activity by this mutant Hel308 protein shown in Figure 5C. Proteins were used at (wild type) 0, 0.2, 0.4, 1.0. 2.0, 5.0, 10, 20, 40 and 80 nM, or for F439A at 0, 0.2, 0.4, 1.0. 2.0, 5.0, 10, 20 nM. The graph was plotted from EMSAs for each protein in duplicate and shows

error bars representing standard error from the mean binding activity. Below the graph are images from an EMSA gel for each protein.

Supplementary Table 1

Relative viability values for *E. coli* strain *dnaE*486 Δ*recQ* transformed by plasmids expressing either no helicase (pEmpty), or expressing RecQ or Hel308 helicases. See also Figures S3 and S10 for summary pictures. Viability was calculated from "spot-test" assays in triplicate grown at the same time from a single starter culture in each case. The mean value for pEmpty (12.3 colonies, at cell dilution of 10^{-5}) was designated as 1.0, from which viabilities of other plasmids were compared to give the values shown below, and plotted in Figures 2 and 5.

Plasmid	**Viability (standard deviation)**
pEmpty	1.0 (+/- 0.16)
pRecQ	0.00067 (+/- 6.2 x 10^{-5})
pHel308	0.000025 (+/- 1.6 x 10^{-5})
pHel308^{K51L}	1.0 (+/- 0.14)
pHel308^{Y460A}	0.045 x 10^{-2}
pHel308^{QYN}	0.069 (+/- 0.006)
pHel308^{F434V}	0.09 (+/- 0.003)
pHel308^{F439A}	0.87 (+/- 1.3 x 10^{-4})

Supplementary Table 2

Plasmids used. Primer sequences used for cloning and mutagenesis are available on request.

Below is the amino acid sequence of MthHel308 used for generating isolated WHD, based on sequence alignment with the crystal structure of *Archaeoglobus* Hel308:

(M)GEVERTTSRIIENRDALYRQIIAQVASGLSGTTEELADF**F**RNT**F**YGYQMVEGPFS DSFGMDSI**QY**EVE**N**ATEYLMRNRILYP(STOP)

Archaeal Hel308 with WHD deleted and replaced by a 22 amino acid “linker” has the above WHD sequence substituted for the following sequence:

PSVAVEVAPGVPAVEEGAVPAV

Below is the amino acid sequence of Human HelQ that was used for generating isolated WHD, based on modeling using the Phyre2 server:

(M)LILQEKDKQQVLELITKPLENCYSHLVQEFTKGIQTLFLSLIGLKIATNLDDIYHFMN GTFFGVQQKVLLKEKSLWEITVESLRYLTEKGLLQKDTI**YK**SEEEV**QY**NFHITKLGRA SFKGTIDLAYCDILYRDLKKGLEGLVLESLLHLIYLTTPYDLVSQ(STOP)

In each case codons for an N-terminal methionine (M) and STOP were introduced into the GeneArt DNA synthesis for cloning, and in bold underlined are amino acids focused on for mutagenesis of these domains.

Name	Description	Reference
pEB310	*Methanothermobacter hel308* cloned into pT7-7 for genetic analysis *in E. coli.*	(1)
pEB431	pET14b cloned *Methanothermobacter hel308* for protein expression and purification.	(2)
pEB422	*Methanothermobacter* mutant *hel308* K51L, created by mutagenesis of pEB310.	(1)
pEB417	*E. coli recQ* cloned into T7-7 for genetic analysis in *E. coli*.	(1)
pEB622	pET14b cloned *Methanothermobacter hel308* winged helix domain. Created from sub-cloning a synthetic sequence from GeneArt.	This work
pEB643	pET14b cloned *Methanothermobacter* full length *hel308* winged helix domain mutant WHD^{QYN}. Created from Q5 mutagenesis of pEB622.	This work
pEB664	pET14b cloned human *helQ* winged helix domain. Created from sub-cloning a synthetic sequence from GeneArt.	This work
pEB665	pET14b cloned human *helQ* winged helix domain mutant Q-WHD^{YK}. Created from Q5 mutagenesis of pEB664	This work
pEB475	pT7-7 cloned *Methanothermobacter* mutant *hel308* F434V, created by Q5 mutagenesis of pEB431.	This work
pEB477	pET14b cloned *Methanothermobacter* mutant *hel308* F434V, created by sub-cloning from pEB475.	This work
pEB444	pT7-7 cloned *Methanothermobacter* mutant *hel308* F439A, created by Q5	This work

	mutagenesis of pEB431.	
pEB447	pET14b cloned *Methanothermobacter* mutant *hel308* F434V, created by sub-cloning from pEB475.	This work

Supplementary Table 3

Summary of the top structural "hits" used by Phyre2 modeling of Human HelQ.

Model Number	PDB template	Confidence	% Identity	Corresponding protein structure
1	5AGA	100	37	Crystal structure of the helicase domain of human polymerase theta in complex with AMP-PNP
2	4F92	100	22	U5 small nuclear ribonucleoprotein kda helicase; Brr2 helicase region
3	4BGD	100	23	Pre-mRna-splicing helicase Brr2
4	2ZJ8	100	28	Putative ski2-type helicase; archaeal DNA helicase Hjm apo state
5	2VA8	100	26	DNA repair helicase SsoHel308

Substrates used for biochemical analysis of Hel308 and HelQ proteins

Oligonucleotides listed below were annealed in appropriate combinations using standard methods described in (1) to create substrates for binding and unwinding assays of Hel308 and HelQ proteins. Unless stated, one oligonucleotide of each substrate had been end labeled with ^{32}P, using T4 polynucleotide kinase treatment with $\gamma^{32}P$ ATP.

Single stranded DNA

5'-
GGAGCTCCCTAGGCAGGATCGTTCGCGACGATGGCCTTCGAAGAGCTCCAGTT
ACGGATACGGATCCTGC

Duplex 70A

5'-
GGAGCTCCCTAGGCAGGATCGTTCGCGACGATGGCCTTCGAAGAGCTCCAGTT
ACGGATACGGATCCTGC

5'-
GCAGGATCCGTATCCGTAACTGGAGCTCTTCGAAGGCCATCGTCGCGAACGAT
CCTGCCTAGGGAGCTCC

Duplex 50

5’-ATCGATAGTCTCTAGACAGCATGTCCTAGCAAGCCAGAATTCGGCAGCGT

5’-ACGCTGCCGAATTCTGGCTTGCTAGGACATGCTGTCTAGAGACTATCGAT

Duplex 33

5’-GAAAAGCAGTCCCCTCGCCTCAGCTACGTTTTC

5’-GAAAACGTAGCTGAGGCGAGGGGACTGCTTTTC

3’ tailed partial duplex

5’-ATCGATAGTCTCTAGACAGCATGTCCTAGCAAGCCAGAATTCGGCAGCGT

5’-GGACATGCTGTCTAGAGACTATCGAT

Flayed duplex

5’-GTCGGATCCTCTAGACAGCTCCATGATCACTGGCACTGGTAGAATTCGGC

5’-CAACGTCATAGACGATTACATTGCTACATGGAGCTGTCTAGAGGATCCGA

1. Guy, C.P. and Bolt, E.L. (2005) Archaeal Hel308 helicase targets replication forks in vivo and in vitro and unwinds lagging strands. *Nucleic Acids Res*, **33**, 3678-3690.
2. Woodman, I.L., Briggs, G.S. and Bolt, E.L. (2007) Archaeal Hel308 domain V couples DNA binding to ATP hydrolysis and positions DNA for unwinding over the helicase ratchet. *J Mol Biol*, **374**, 1139-1144.

S1

```
Human-Hel308            VAKKTIESSSNDLGPFYSLPSKVRDLY-AQFKGIEKLYEWQHTCLTLNSVQERKNLIYSL   359
Methanothermobacter     ---------------MKSLPPEMRQILGDCYPHIRELNPAQRSAIEAGYLESEDNYIIAI   45
Sulfolobus              LEWMPIED------LK--LPSNVIEIIK--KRGIKKLNPPQTEAVKKGLLEG-NRLLLTS   53
Archaeoglobus           ---MKVEE------LAESISSYAVGILK--EEGIEELFPPQAEAVE-KVFSG-KNLLLAM   47
Pyrococcus              ---MRVDE------LR--VDERIKSTLK--ERGIESFYPPQAEALKSGILEG-KNALISI   46
                                     :             *..:   *  .:    ..  .. : :

Human-Hel308            PTSGGKTLVAEILMLQELLCCRKDVLMILPYVAIVQEKISGLSS---FGIELGFFVEEYA   416
Methanothermobacter     PTASGKTLLGIIAALKTV-MEGGRVIYTVPLLSIQNEKIKEFRKLEEHGIRVGKDPR---   101
Sulfolobus              PTGSGKTLIAEMGIISFLLKNGGKAIYVTPLRALTNEKYLTFKDWELIGFKVAMTSGDYD   113
Archaeoglobus           PTAAGKTLLAEMAMVREA-IKGGKSLYVVPLRALAGEKYESFKKWEKIGLRIGISTGDYE   106
Pyrococcus              PTASGKTLIAEIAMVHRILTQGGKAVYIVPLKALAEEKFQEFQDWEKIGLRVAMATGDYD   106
                        **..****:. :  :          :   *  ::  **   : .    *:.:.

Human-Hel308            GSKGRFPPTKRREKKSLYIATIEKGHSLVNSLIETGRIDSLGLVVVDELHMIGEGSRGAT   476
Methanothermobacter     -------------TSDIAVMVFESFDSLTRF--SWNILREVDLLIVDEFHMIGEYTRGPV   146
Sulfolobus              TDDAWL------KNYDIIITTYEKLDSLWRH--RPEWLNEVNYFVLDELHYLNDPERGPV   165
Archaeoglobus           SRDEHL------GDCDIIVTTSEKADSLIRN--RASWIKAVSCLVVDEIHLLDSEKRGAT   158
Pyrococcus              SKDEWL------GKYDIIIATAEKFDSLLRH--GSSWIKDVKILVADEIHLIGSRDRGAT   158
                                  .: : . *. .** .       :  :  .: **:* :..  ** .

Human-Hel308            LEMTLAKILYTSKTTQIIGMSATLNNVEDLQKFLQAEYYTSQFRPVELKEYLKINDTIYE   536
Methanothermobacter     IESAITRARTLNPSVRIVALSATLSNMDEIAGWLDARVVEHDYRPVPLHREVLDTEMFG-   205
Sulfolobus              VESVTIRA----KRRNLLALSATISNYKQIAKWLGAEPVATNWRPVPLIEGVIYPERKK-   220
Archaeoglobus           LEILVTKMRRMNKALRVIGLSATAPNVTEIAEWLDADYYVSDWRPVPLVEGVLCEGTLE-   217
Pyrococcus              LEVILAHML---GKAQIIGLSATIGNPEELAEWLNAELIVSDWRPVKLRRGVFYQGFVT-   214
                        :*    :        .::.:***  *  ::  :* *     ::*** * . :

Human-Hel308            VDSKAENGMTFSRLLNYKYSDTLKKM-DPDHLVALV-TEVIPNYSCLVFCPSKKNCENVA   594
Methanothermobacter     ----VR----E---------------KNDVVLKVLERSLEDGSQTLAFVSTRRFTESLA   241
Sulfolobus              ----KEYNVIFK-------DNTTKKVHGDDAIIAYTLDSLSKNGQVLVFRNSRKMAESTA   269
Archaeoglobus           ----LFDGAFST-------S-------RRVKFEELVEECVAENGGVLVFESTRRGAEKTA   259
Pyrococcus              ----WEDGSID---------------RFSSWEELVYDAIRKKKGALIFVNMRRKAERVA   254
                                                          :     * *   ::  *  *
```

S1 (cont.)


Human-Hel308
Methanothermobacter
Sulfolobus
Archaeoglobus
Pyrococcus
alpha helix-20

S1 (cont.)

```
Human-Hel308              NRLYLSFVLYTLLKETNIWTVSEKFNMPRGYIQNLLTGTASFSSCVLHFCEELEEFWVYR   992
Methanothermobacter       NEEATAAALIEWINERTEYEIENAFHVYAASTRRSAYEASKIVKFFGKICEIMGVYRH-S   617
Sulfolobus                NALKVALIMKDWMDEVDEDTILSKYNIGSGDLRNMVETMDWLTYSAYHLSRELKLNEH-A   638
Archaeoglobus             SEVKTALCLKDWIEEKDEDEICAKYGIAPGDLRRIVETAEWLSNAMNRIAEEVGNTSV-S   617
Pyrococcus                RAFKTALVLLAWINEVPEGEIVEKYSVEPGDIYRIVETAEWLVYSLKEIAKVLGAYEI-V   627
                               :  :   :.*     :   : :  .   .       :     .:.. :

Human-Hel308              ALLVELTKKLTYCVKAELIPLM-EVTGVLEGRAKQLYSAGYKSLMHLANANPEVLVRTID   1051
Methanothermobacter       SQLEILSARLYYGVKEDAIPLVVGVRGLGRVRARKIIKTF----GEDLRHVREDELKRID   673
Sulfolobus                DKLRILNLRVRDGIKEELLELV-QISGVGRKRARLLYNNGIKELGDVVMNPDKVKNLLGQ   697
Archaeoglobus             ----GLTERIKHGVKEELLELV-RIRHIGRVRARKLYNAGIRNAEDIVRHREKVASLIGR   672
Pyrococcus                DYLETLRVRVKYGIREELIPLM-QLPLVGRRRARALYNSGFRSIEDISQARPEELLKI-E   685
                               *  ::   :: : : *:  :  : . **: : .       .      :

Human-Hel308              HLSRRQAKQIVSSAKMLLHEKAEALQEEVEELLRLPSDFPGAVASSTDKA     1101
Methanothermobacter       GIGPKMAGAIRRYCERF--------------------------------     690
Sulfolobus                KLGEKVVQEAARLLNRFH-------------------------------     715
Archaeoglobus             GIAERVVEGIS------VK-SLNPES-----------------------     691
Pyrococcus                GIGVKTVEAIFKFLGKNVKISEKPRKSTLDYFLKS---------------     720
                           :. : .
```

S2

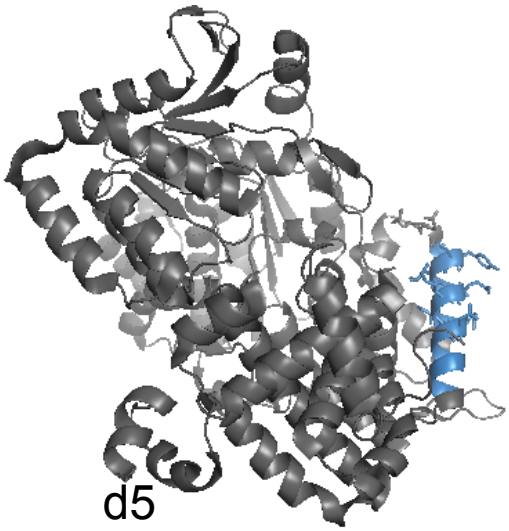

PfuHel308

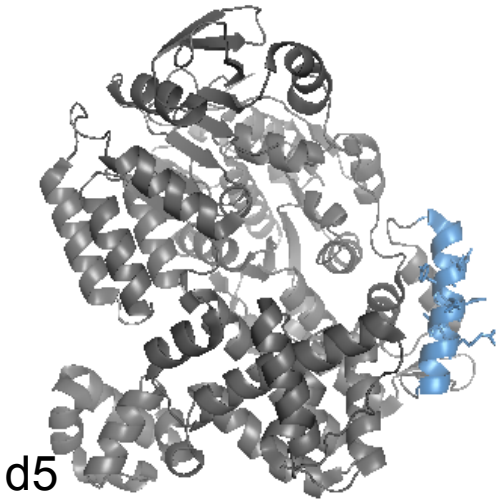

SsoHel308

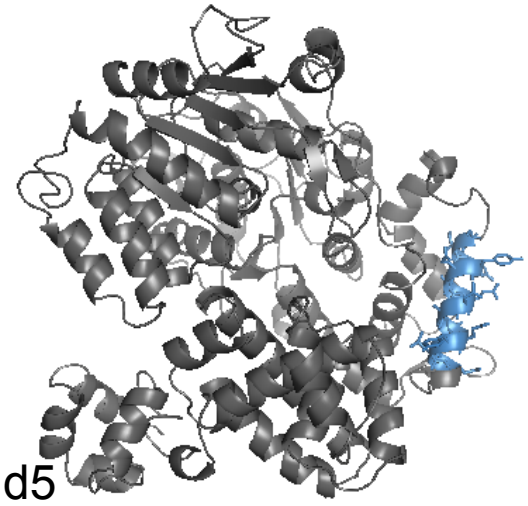

MthHel308 (model)

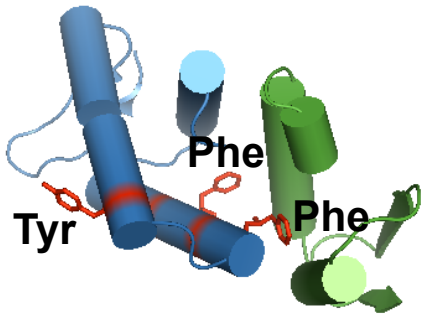

PfuHel308

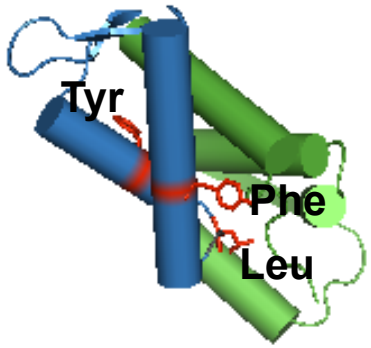

SsoHel308

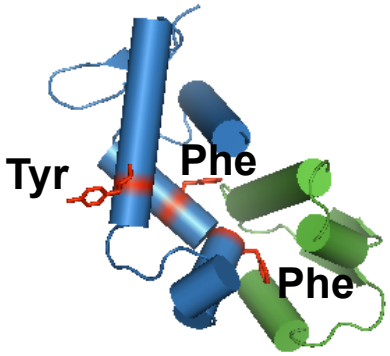

MthHel308 (model)

S3

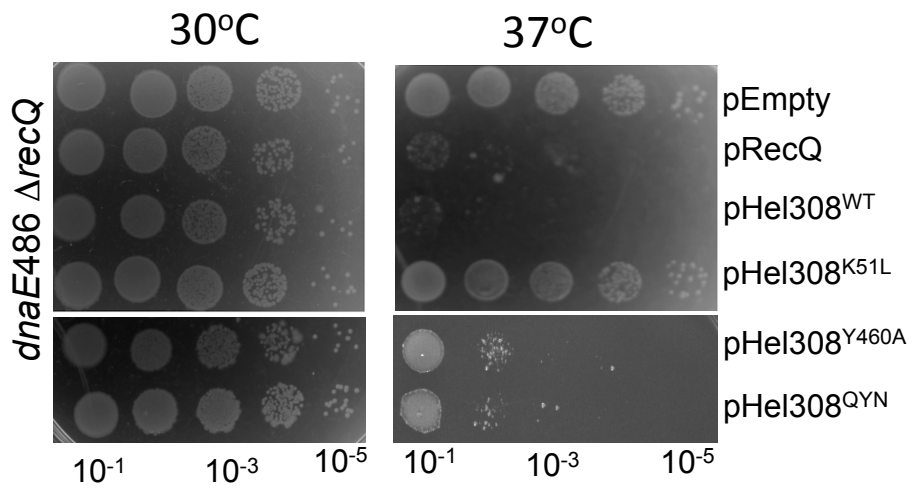
30ºC
37ºC
dnaE486 ΔrecQ
pEmpty
pRecQ
pHel308WT
pHel308K51L
pHel308Y460A
pHel308QYN
10-1
10-3
10-5
10-1
10-3
10-5

S4

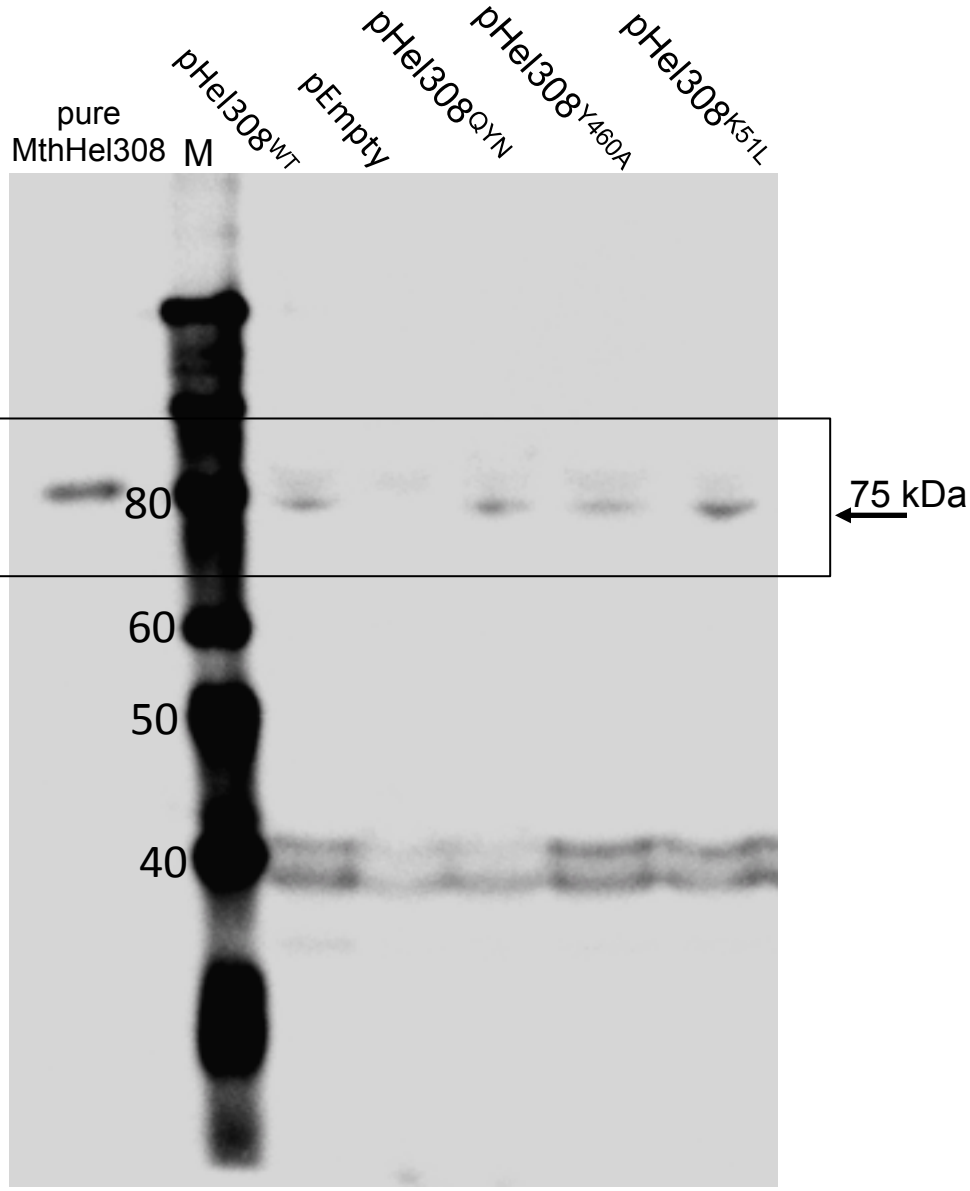
pure MthHel308
M
pHel308WT
pEmpty
pHel308QYN
pHel308Y460A
pHel308K51L
80
60
50
40
75 kDa

Figure 2

S5

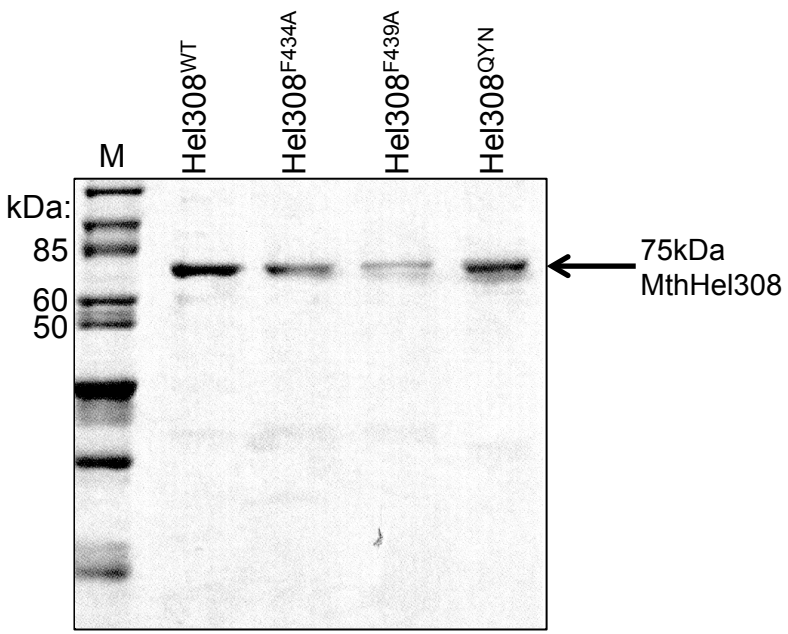
M
Hel308WT
Hel308F434A
Hel308F439A
Hel308QYN
kDa:
85
60
50
75kDa
MthHel308

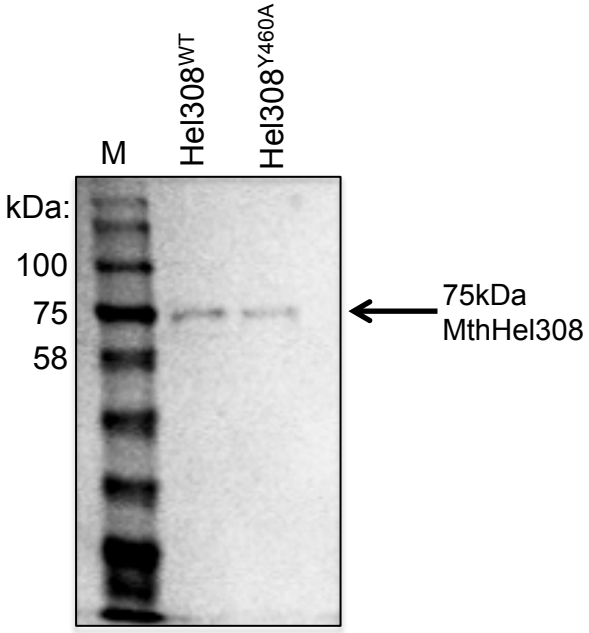
M
Hel308WT
Hel308Y460A
kDa:
100
75
58
75kDa
MthHel308

S6

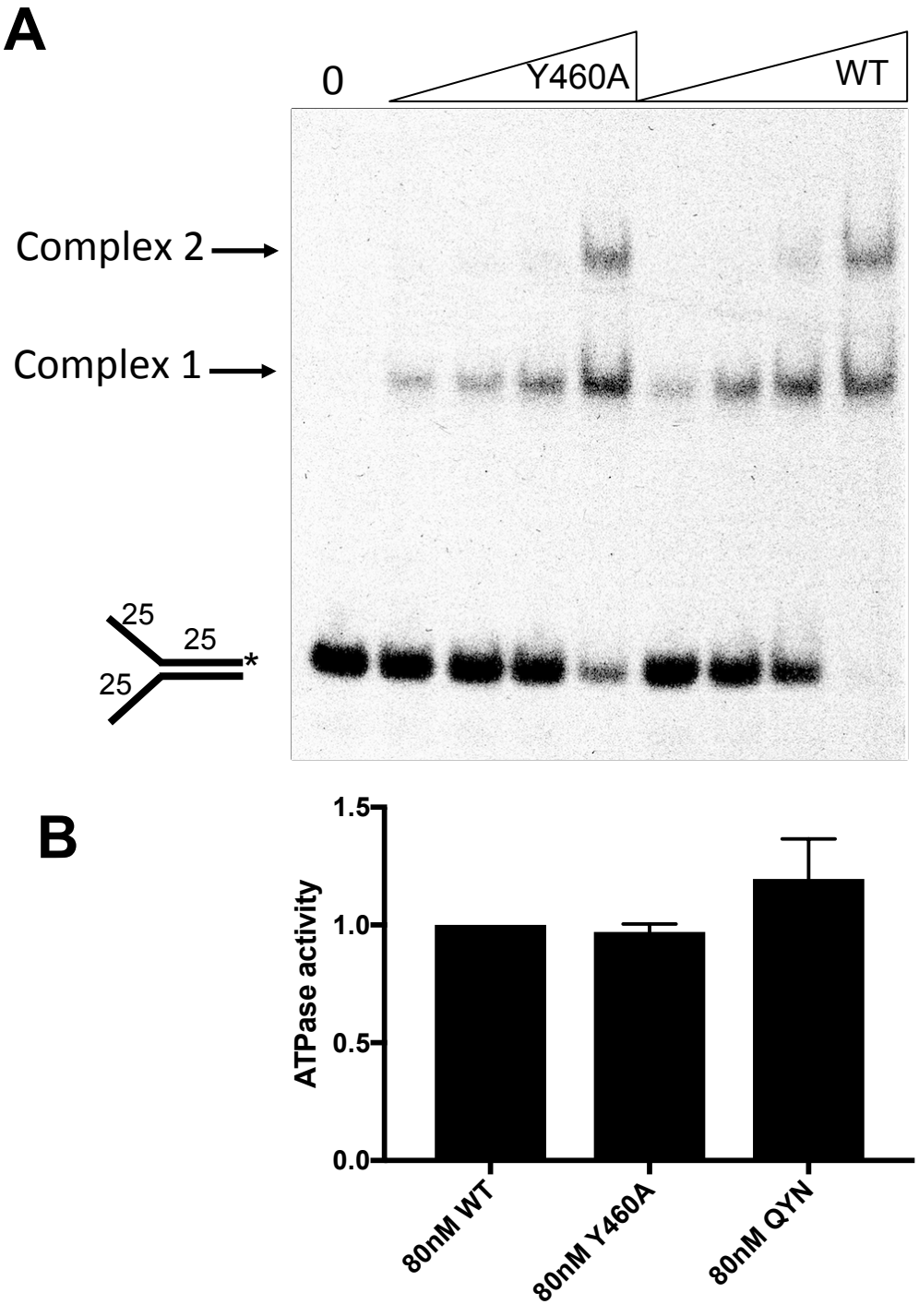
A
0
Y460A
WT
Complex 2
Complex 1
25
25
25
*
B
ATPase activity
1.5
1.0
0.5
0.0
80nM WT
80nM Y460A
80nM QYN

S7

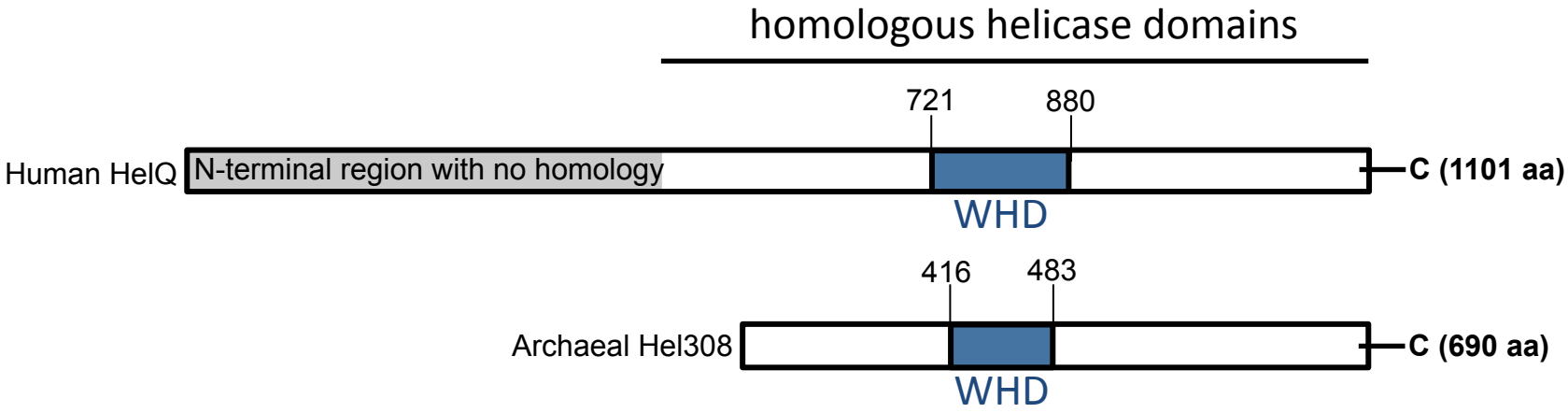
homologous helicase domains
721
880
Human HelQ
N-terminal region with no homology
C (1101 aa)
WHD
416
483
Archaeal Hel308
C (690 aa)
WHD

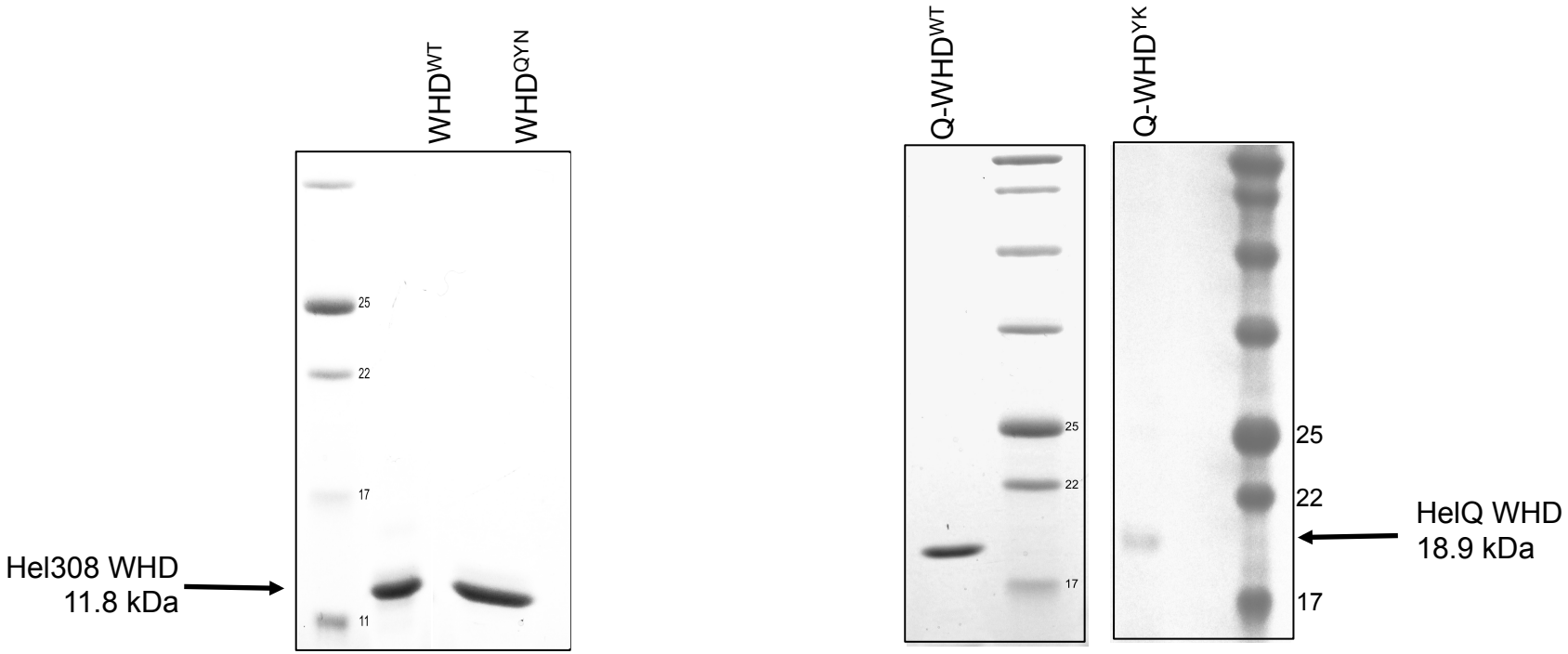
WHD^WT
WHD^QYN
25
22
17
11
Hel308 WHD
11.8 kDa
Q-WHD^WT
Q-WHD^YK
25
22
17
25
22
17
HelQ WHD
18.9 kDa

S8

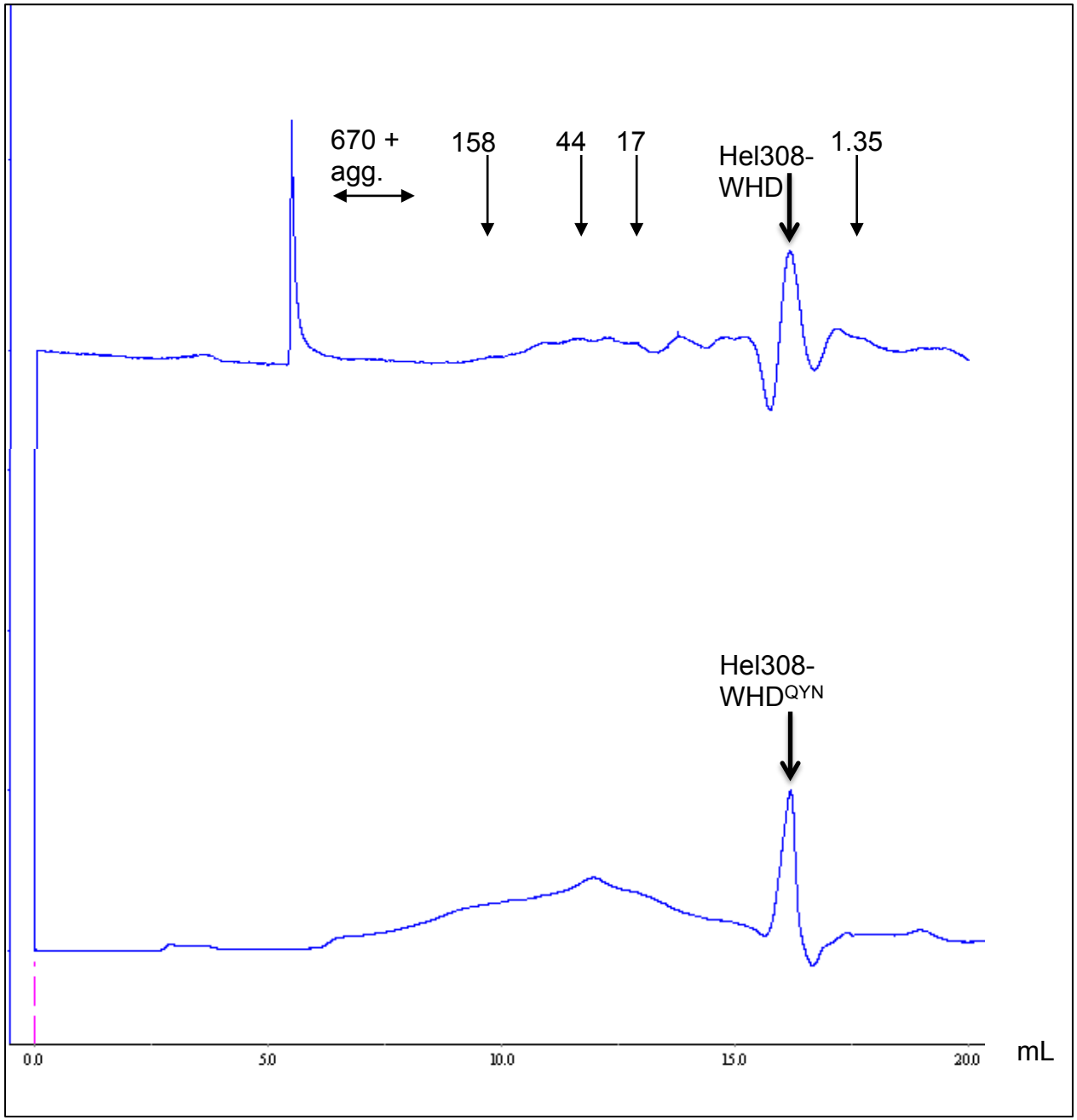
670 +
agg.
158
44
17
Hel308-
WHD
1.35
Hel308-
WHD^QYN
0.0
5.0
10.0
15.0
20.0
mL

S9

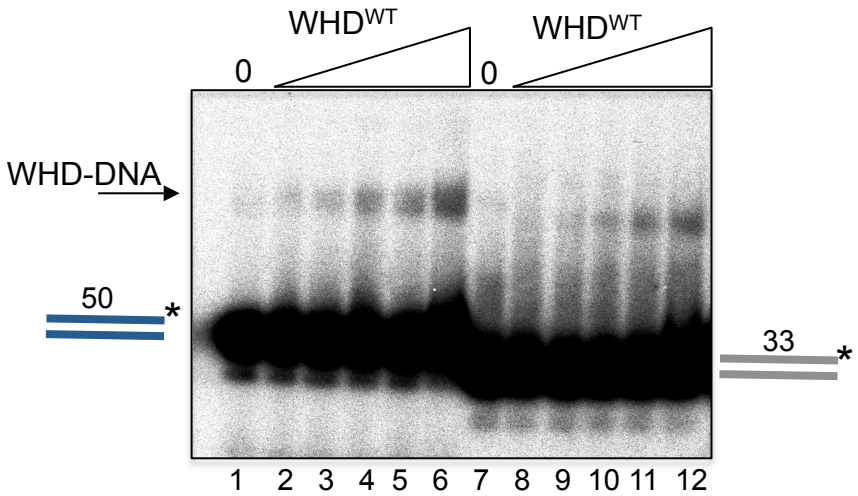

S10

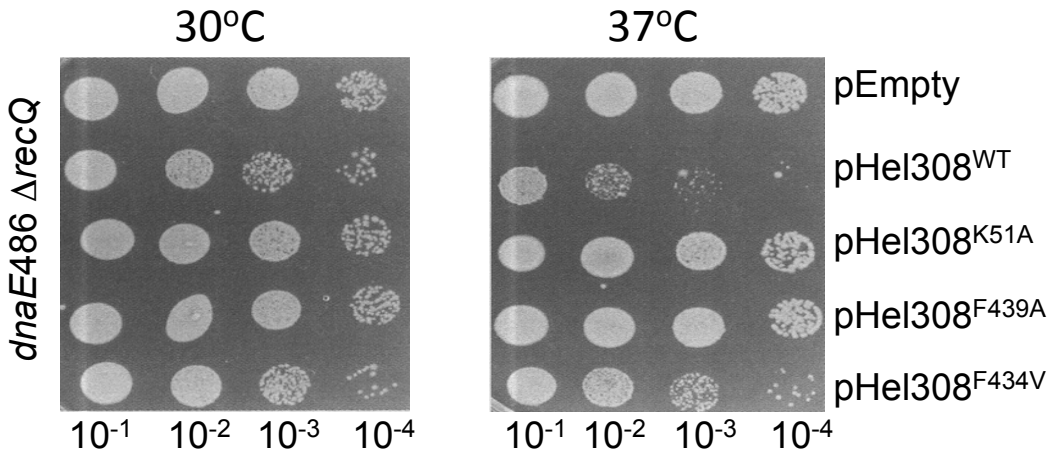
30ºC
37ºC
dnaE486 ΔrecQ
pEmpty
pHel308WT
pHel308K51A
pHel308F439A
pHel308F434V
10-1 10-2 10-3 10-4
10-1 10-2 10-3 10-4

S11

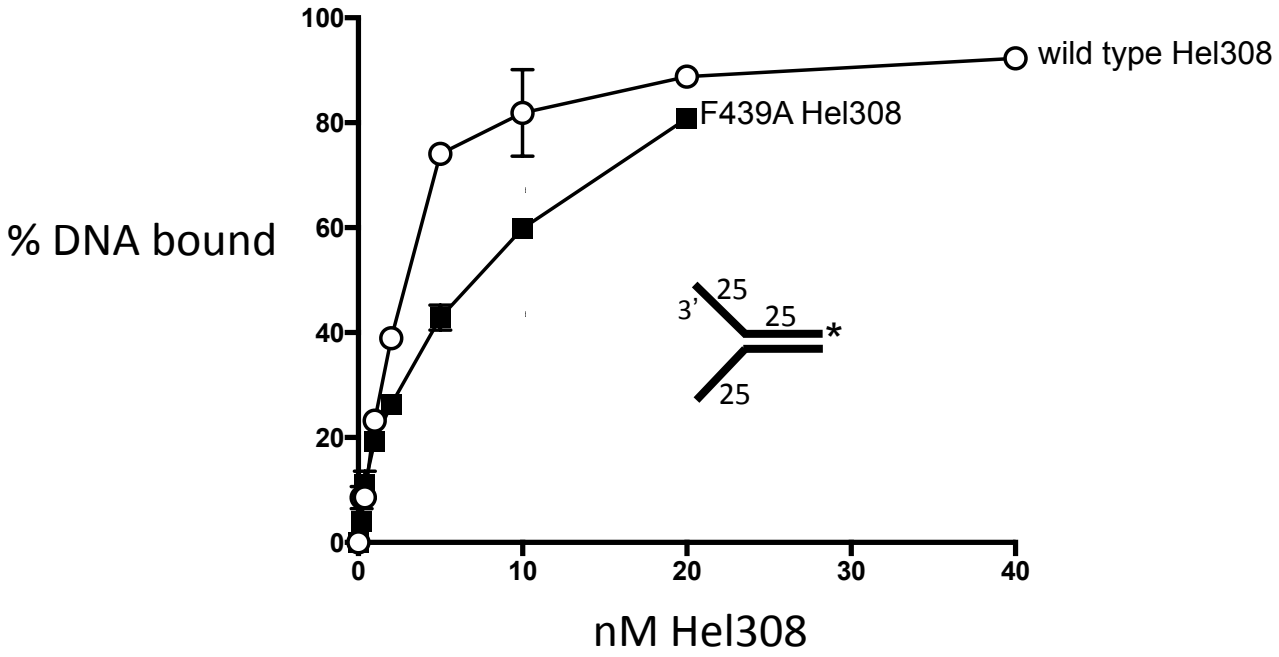
100
80
60
40
20
0
% DNA bound
0
10
20
30
40
nM Hel308
wild type Hel308
F439A Hel308
3'
25
25
25
*

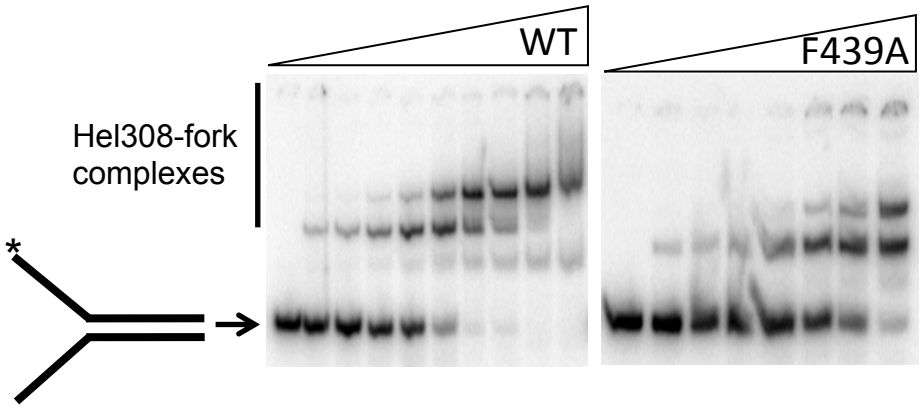
WT
F439A
Hel308-fork
complexes
*